

# TRANSITION METAL OXIDES BASED SUPERCAPACITOR

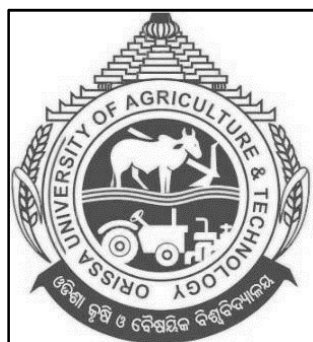
A

Thesis Submitted To  
Odisha University of Agriculture and Technology, Bhubaneswar  
In Partial Fulfilment of The Requirement of The Degree of  
MASTER OF SCIENCE IN CHEMISTRY

By

RUDRA RATIKANTA POTHAL

Admission No.: 06CHEM/19



DEPARTMENT OF CHEMISTRY

COLLEGE OF BASIC SCIENCE AND HUMANITIES  
ODISHA UNIVERSITY OF AGRICULTURE & TECHNOLOGY  
BHUBANESWAR- 751003  
2021

Pothal, R, R. M.Sc. (CHEMISTRY) THESIS -(2021)  
Transition Metal –Oxides based Supercapacitor :

# **TRANSITION METAL-OXIDES BASED SUPERCAPACITORS**

A

Thesis Submitted To

Orissa University of Agriculture and Technology, Bhubaneswar

In Partial Fulfillment of The requirement of The Degree of

MASTERS OF SCIENCE IN CHEMISTRY

BY

RUDRA RATIKANTA POTHAL

Admission No.: 06 CHEM/19



**DEPARTMENT OF CHEMISTRY**

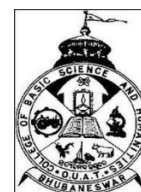
**COLLEGE OF BASIC SCIENCE AND HUMANITIES**

**ORISSA UNIVERSITY OF AGRICULTURE AND TECHNOLOGY,  
BHUBANESWAR- 751003**

**2021**



ORISSA UNIVERSITY OF AGRICULTURE AND TECHNOLOGY  
DEPARTMENT OF CHEMISTRY  
COLLEGE OF BASIC SCIENCE AND HUMANITIES



Dr. (Mrs.) Swarnabala Jena  
Assistant Professor  
Department of Chemistry

### **CERTIFICATE – I**

This is to certify that the thesis entitled, **“TRANSITION METAL-OXIDES BASED SUPERCAPACITORS”** submitted in partial fulfillment of the requirements for the award of the degree of Master of Science in **CHEMISTRY** to the Orissa University of Agriculture and Technology, Bhubaneswar, is a faithful record of bonafide research work carried out by **RUDRA RATIKANTA POTHAL**, **Adm No: 06- CHEM/19** under my guidance and supervision and that no part of thesis has been submitted for any degree or diploma or published in any form.

It is further certified that the help and sources of information availed of during the course of study have been duly acknowledged.

Place: Bhubaneswar  
Date:

Dr. Swarnabala Jena  
Assistant Professor,  
Department of Chemistry  
CHAIRMAN  
ADVISORY COMMITTEE

## **CERTIFICATE-II**

This is to certify that the thesis entitled “**TRANSITION METAL-OXIDES BASED SUPERCAPACITOR**” submitted by RUDRA RATIKANTA POTHAL to Orissa University of Agriculture and Technology , Bhubaneswar in partial fulfilment of the requirements for the award of the degree of **MASTER OF SCIENCE IN CHEMISTRY** has been approved by the students’ Advisory Committee .

### **ADVISORY COMMITTEE:**

**CHAIRMAN: Dr.(Mrs.)Swarnabala Jena**

Assistant Professor  
Department of Chemistry  
College of Basic Science and Humanities  
O.U.A.T., Bhubaneswar-3

---

### **MEMBERS:**

**Dr.(Mrs.)Nandita Swain**

Professor and Head  
Department of Chemistry  
College of Basic Science and Humanities  
O.U.A.T., Bhubaneswar-3

---

**EXAMINER**

---

## ACKNOWLEDGEMENT

At the outset I take this opportunity to acknowledge all the persons whose help and support has made me complete this work successfully.

I express my sincere reverence, obligation & deepest sense of gratitude to my guide Dr. (Mrs) Swarnabala Jena, Assistant professor, Department of Chemistry, College of Basic Science and Humanities, O.U.A.T, Bhubaneswar for her keen supervision, help in every aspect, scholastic suggestions, constructive criticisms, whole hearted cooperation and encouragement throughout the entire course of investigation and preparation of this manuscript.

I express my sincere obligation to Dr. Choudhury Suryakanta Mishra, Director, College of Basic Science and Humanities, Dr.(Mrs.) Nandita Swain, Professor and Head, Department of Chemistry and to all the faculties and Staff of the department of chemistry, College of Basic Science and Humanities, OUAT, Bhubaneswar, for their interest and encouragement in my work.

. I am also thankful to my parents for their constant inspiration and unfailing support towards the completion of this work

Finally I pay my obeisance at lotus feet of lord JAGANNATH for his blessings to be an asset to do my research work.

Place: Bhubaneswar

( Rudra RatikantaPothal )

Date:

# CONTENT

---

CHAPTER NO.	DESCRIPTION	PAGE NO.
1	INTRODUCTION	1-7
2	TRANSITION METAL OXIDES USED AS ELECTRODE MATERIALS	7-24
3	CONCLUSION AND SUGGESTION	24
4.	REFERENCE	24-33

---

## LIST OF FIGURES

---

FIGURE NO.	PARTICULARS	PAGE NO.
1	COMPONENTS OF SUPERCAPACITOR	2
2	RAGONE PLOT	3
3	PICTURE OF CAPACITOR	3
4	PICTURE OF SUPERCAPACITOR	4
5	WORKING OF SUPER CAPACITOR	4
6	TYPES OF SUPER CAPACITOR	5
7	CV – CURVE	7
8	TEM AND CV-CURVE OF RuO <sub>2</sub> -CARBON COMPOSITE	9
9	COMMERCIAL SUPERCAPACITOR	10
10	CRYSTAL STRUCTURE OF MnO <sub>2</sub>	11
11	TEM & SEM PICTURE OF MnO <sub>2</sub>	13
12	FORMATION OF Mn <sub>3</sub> O <sub>4</sub>	14
13	SYNTHESIS OF MnO <sub>2</sub>	14
14	CRYSTAL STRUCTURE OF Fe <sub>2</sub> O <sub>3</sub>	17
15	TEM ,SEM&GRAPHS OF Fe <sub>2</sub> O <sub>3</sub>	18
16	N <sub>2</sub> ADSORPTION – DESORPTION ISOTHERM	22
17	CV-CURVE OF NiMnO <sub>4</sub> COMPOSITE	23
18	COMPARISON OF SPECIFIC CAPACITANCE	24

## ABBREVIATIONS AND SYMBOLS USED

SS:	-	Stainless steel
SHE:	-	Standard hydrogen electrode.
AC:	-	Activated Carbon
SC:	-	Specific Capacitance
CV:	-	Cyclic-Voltametry
et al.,	-	et alebi (and others)
etc	-	et cetra
Fig	-	Figure
g	-	Gram
ml	-	Millilitre
XRD	-	X-ray diffraction

# TRANSITION METAL – OXIDE BASED SUPERCAPACITOR

## ABSTRACT

Today's world is in greater threat due to global warming and increasing energy demand due to extensive use of fossil fuel. In order to fulfil the hunt for increasing energy demand researchers triggered for search of generation of sufficient amount of energy in a greener method. Hence, development of various high performance energy storage devices, such as fuel cells, batteries, and supercapacitors has gained much attention in recent years. In order to meet the future energy demand, amongst the previously mentioned energy storage devices, much attention has been given towards the development of high-performance supercapacitors as they have several advantages, such as fast charging and discharging ability, longer cyclic lifespans, and wide operating temperature ranges over the fuel cell and battery. In supercapacitors charge storage occurs either by ion adsorption or redox reaction. This classifies the super capacitors into electrical double layer (EDLC) and pseudo capacitors. The synthesis of metal oxide has drawn much attention due to their distinguished physical and chemical properties. Metal oxides with unique porous structure, high surface area and easy access of the electrolyte ions into the electrode surface through the pores of active materials make them superior material for supercapacitor applications. Along with this distinguished properties metal oxides have attractive performances for fabricating various supercapacitor devices in a broad voltage window. The transition metal oxide materials, due to their abundance reserves, environmental benignity, easy approachability has earned greater attention along with other fascinating characters such as their diverse constituents, large surface area and high theoretical specific capacitance. They play a central part of the electrodes of the electrochemical supercapacitors and improves capacitance by adjusting their defects at surface / interfaces under nano scale range and increases energy density. However, low electrical conductivity, uncontrollable volume expansion, and slow ion diffusion in the bulk phase hinders their practical application. Hence, bimetallic oxide materials are highly useful in order to overcome the poor electric conductivity of single metal oxide materials to achieve high capacitance and raises the energy density at capacitor level. In this review some metal oxide both metallic and bimetallic have been discussed along with their energy storage mechanism, the influence on chemical composition, structural features, electro conductivity, morphologies, and various electrolytes in the electrochemical behaviour are discussed so that in near future researchers find a new direction on the future of metal oxide based supercapacitors.

## INTRODUCTION

In the recent decades, environmental pollution accompanied with energy crises is the great issues for researchers. Now days the consumption limit of fossil fuel is too high that the earth accelerates towards the path of darkness in the near future. The environmental pollution also increases owing to the depletion level of fossil fuel reservoir. The increasing combustion of fossil fuel results in the production of gases like CO<sub>2</sub>, NO<sub>2</sub>, and CH<sub>4</sub> etc., which absorbs the solar radiation from the atmosphere and makes the earth hotter. According to NASA's survey at GODDARD institute , the average temperature of earth increases by 0.8°C due to rapid industrialisations and this small change in temperature causes melting of polar ice caps and glaciers which in turn causes flooding and rising of sea level at the coastal regions[1-3]. This ultimately threatens the survival of life on earth. Hence, in order to maintain the sustainability of life on earth and their life standards, there is a need of energy sources like solar wind etc.that gives sufficient energy for survival. However, these natural energy sources face various climatic issues and cannot fulfil sufficiently our demands for energy. This stimulates the scientific community for the search of alternative energy storage systems that can reduce the use of fossil fuels.

many energy storage devices such as battery, capacitors, fuel cells and super capacitors are used today to store energy. Amongst, super capacitor or electrochemical capacitor is considered as an excellent energy storage device due their high power densities, long life span and short charging time .The more energy density and life line of the super capacitors mainly depends upon the electrode materials used and the stability of electrolytes [1].In 1978, a super capacitor introduced by NCE, which is used to provide the power back up for the computes [4]. Generally, the electrode materials used for super capacitor should possess various physio chemical properties such as high conductivity, high surface area, amorphous, good corrosion resistance, high temperature stability and relatively low cost. Several materials such as transition metal oxides, carbon aerogels, and graphene composites etc. are used as electrode materials for super capacitors. Among them, transition metal oxides are considered as promising candidate as electrode material for super capacitor due to their easy abundance, environmental benignity, easy approachability , low cost , high surface area, chemically non-hazardous and high theoretical specific capacitance[ 5-7 ] . RuO<sub>2</sub> is the best

transition metal oxides for this purpose, but the technical huddles associated with it is high expensive [8]. Various TMO  $\text{NiFe}_2\text{O}_4$ , and  $\text{BiFeO}_3$  are useful for super capacitive electrode materials [4, 9-14]. The design of metal oxides depends in terms of their composition. The fabrication of the nanostructure mainly based on the electrical conductivity and oxygen vacancies of the metal oxides.. For better electrical conductivity binary metal oxides shows efficient electrical conductance than single metal oxide. For example, electrodes of  $\text{NiCo}_2\text{O}_4$  show more electrical conductivity than the individual one  $\text{NiO}$  and  $\text{Co}_3\text{O}_4$ . By experiment, It is seen that the addition Ni with  $\text{Co}_3\text{O}_4$  increases the electrical conductivity from  $3.1 \times 10^{-5} \text{ s cm}^{-1}$  to  $0.1 \text{ s cm}^{-1}$  [15-17]. Again, the metal oxides having porous structure can easily transport the metal ions so that electrical conductivity increases. The oxygen vacancies in the metal oxides makes the electrodes porous and increases the surface area due to which electrical conductivity along with storage capacity increases which can be given by the formula  $C \propto A/D$  [ 18 – 21] . It is proved that  $\text{MoO}_{3-x}$  has two times larger electrical conductivity than  $\text{MoO}_3$ [22].

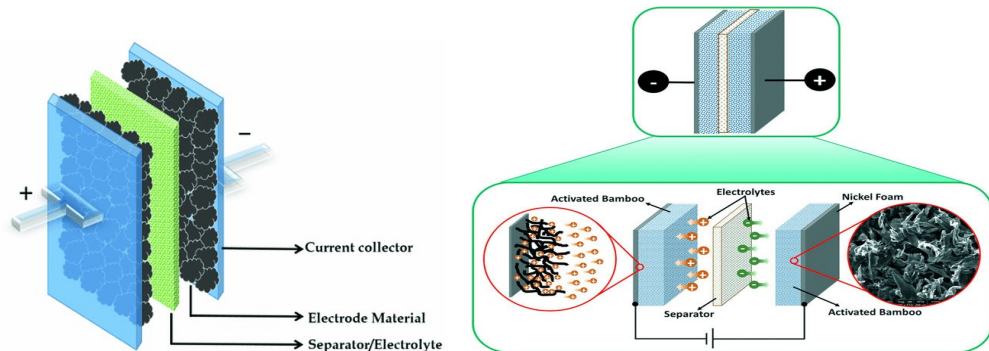


**Fig 1- diagram of supercapacitor and its components.**

Supercapacitors are also known as ultra-capacitors, double layer capacitors or electrochemical capacitors. They utilize large surface area and thinner dielectrics to achieve greater power density than that of batteries and greater capacitances with higher energy density than that of conventional capacitors[23-29]. Super capacitor reaches 20 times P.D (>10 KILOWAAT PER KG) and good life cycle (>105 cycles) than that of batteries, also it can be charged/discharged rapidly[30, 31]. It is used in variety energy storage device. Fig. 2 indicates the comparison of specific energy and specific power.. [32-33]

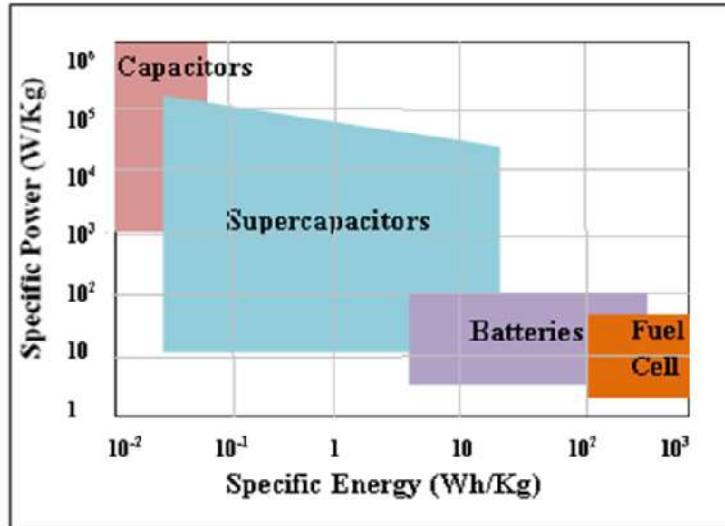


**Fig 2** Ragone plot: Specific Energy Vs Specific Power Plot

In this review article, we have presented the Basic idea about capacitor, super capacitor working of supercapacitor, types of supercapacitor, electrode material, electrolytes used and transition metals used as electrode materials like RuO<sub>2</sub>, MnO<sub>2</sub>, Mn<sub>3</sub>O<sub>4</sub>, Fe<sub>2</sub>O<sub>3</sub>, Fe<sub>3</sub>O<sub>4</sub>, NiO etc

### Capacitor:

Capacitor is an electric component, which is used to store charge in the form of electric potential. Capacitor consists of two parallel plates separated by small distance in few millimeter. Here the Amount of charge store in the capacitor is known as capacitance, it depends upon the dimensions of the capacitor. The increase and decreasing of capacitance depends upon dimension of the capacitor and materials used in it. When the capacitor is attached across the battery an electric field develops across the dielectric causing +ve charge on one plate and -ve charge on another plate. [wikipedia]

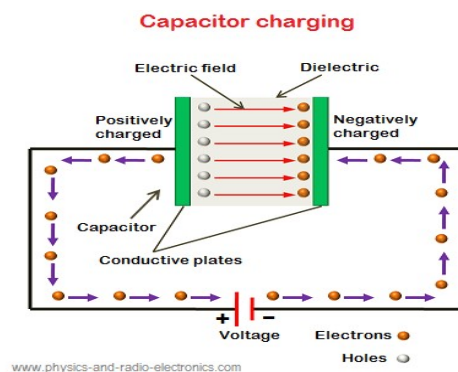


**Fig 3-** picture of capacitor

## Super capacitor

Supercapacitors are capacitors that have a higher capacitance and energy density than ordinary capacitors. By delivering great power performance in a small design, super capacitors can bridge the gap between ordinary capacitors and batteries. It is made up of two electrodes, an electrolyte in the middle, and a membrane that separates them.[Wikipedia]

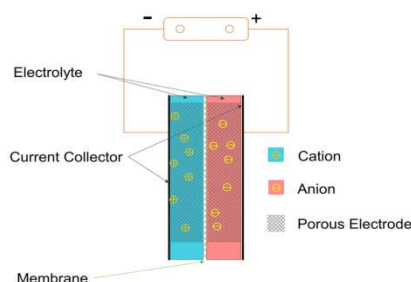


fig 4 – picture of super capacitor

## Working of supercapacitors:

A supercapacitor consists of one porous membrane, which separates the +ve and -ve plate is called separators. The two electrodes are electrically connected with ionic liquid called electrolyte. When the voltage is applied to the +ve electrode it attracts the -ve ions from the electrolyte. Similarly when the voltage is applied to the -ve electrode it attracts the +ve ions from the electrolyte. These ions are stored near the surface of the electrodes due to which the distance between the electrodes decreases. Due to decrease in distance, the capacitance becomes very large which can be shown by the formula  $C \propto A/D$ . [wikipedia]

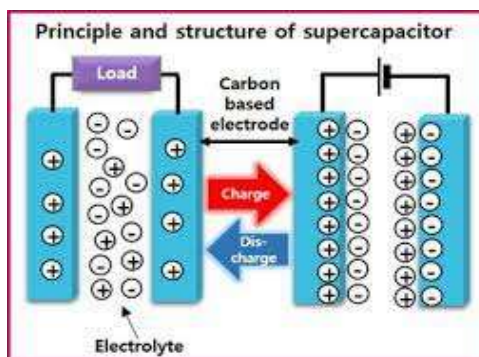


Fig 5 – Picture of working of supercapacitor

## Types of super capacitors :

Normally based on mechanism of energy storage and cell configuration the supercapacitors are divided into 3 types such as: (i) Electric Double-Layer Capacitors (EDLC's), (ii) Pseudocapacitors and (iii) Hybrid capacitors.

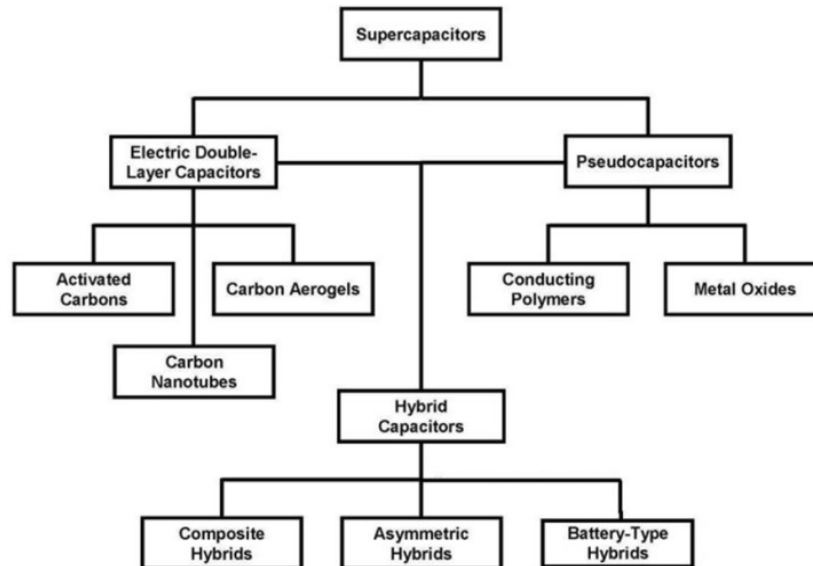


Fig -6 variety types of super capacitor

## Electric double layer capacitor (EDLC) :

EDLCs are made up of two porous carbon-based electrode materials separated by an insulator. The energy charge is stored in a non-faradaic way here, with the charge storage process relying on the buildup of electrostatic charge at the electrode-electrolyte interface. Because carbon nanomaterials have distinctive structures with large surface areas, higher electrical conductivity, and excellent chemical and mechanical durability, activated carbon is the most popular electrode material [34, 35]. The construction of EDLCs is identical to that of ordinary capacitors, with the exception that the dielectric is replaced with electrolyte. The positive and negative ions of the battery are charged during the charging process. Negative and positive electrodes separate and adsorb electrolyte, respectively [36]. EDLC can store much more charge than traditional capacitors. [37]

## Pseudocapacitor:

Pseudo capacitor that stores energy through a reversible redox process or a Faradic reaction [38]. In comparison to EDLCs, pseudo-capacitors store charge electrostatically. In Pseudocapacitors, faradaic charge transfer occurs at the electrode-electrolyte interface. Due to Faradic process, it has more energy density and capacitance than EDLC. Transition metal oxides and conducting polymers are primarily utilized as pseudocapacitor electrodes in pseudo capacitors [39-46].

## Hybrid supercapacitor:

Hybrid supercapacitors combine the properties of both EDLCs and pseudocapacitors to create a third type of supercapacitor. The electrodes of hybrid supercapacitors are made up of a mix of EDLC (CARBON, carbon nanotubes, etc.)

and pseudocapacitive (transition metal oxides and conducting polymers) materials). Because hybrid supercapacitors combine EDLC and pseudo capacitors, they provide a high energy density and quick charging rate in a single cell. Due to the larger operating voltage of an organic electrolyte and the excellent specific capacity of the battery type electrode, combining two distinct electrodes results in more energy storage.

There are three types of hybrid capacitors based on configurations of electrodes (a) composite hybrid capacitors, (b) asymmetric hybrid capacitors and (c) battery-type hybrid capacitors [47-54].

### **Electrolytes:**

Aside from electrodes, the electrolyte is another essential component that can have a significant impact on the electrochemical performance of a supercapacitor device. Electrolyte can be found both inside the separator and within the active material layers. High ionic concentration, low resistivity, low viscosity, and other key parameters for an electrolyte might impact the power deposition. Aqueous electrolytes, organic electrolytes, and ionic electrolytes are the three types of electrolytes often utilised in supercapacitors. H<sub>2</sub>SO<sub>4</sub>, KOH, Na<sub>2</sub>SO<sub>4</sub>, HCl, NaCl, and NH<sub>4</sub>Cl aqueous solution,. Aqueous electrolyte supercapacitors may have a greater charge storage capacity.. Acetonitrile and propylene carbonate (PC) are two popular solvents for organic electrolytes. Aqueous electrolyte is utilised as a supercapacitor in some situations when cost is more essential than performance.(55-58)

### **Electrode materials supercapacitor(sc):**

Carbon, metal oxide, and conductive polymer are some of the electrode materials that may be utilised in supercapacitors. Carbon materials with capacitive behaviour, including as carbon, carbon nanotubes), multi-walled (MWCNTs), single-walled (SWCNTs), and graphene, are commonly used as electrodes for EDLC. Metal oxide, on the other hand, especially supercapacitor. There are now a large range of materials available for super- capacitors that were produced using various techniques, particularly to obtain varied morphologies and porous architectures. Transition metal oxides such as ruthenium, manganese, nickel, cobalt, tungsten, and vanadium are among the materials. Meanwhile, conducting polymers of polyaniline (PANI), polypyrrole (PPy), and poly(3,4-ethylene dioxytetrafluoroethane). Although many synthesis methods have been developed to prepare the above materials, they can be grouped into the following categories: sol-gel synthesis, chemical precipitation, hydrothermal/ solvothermal synthesis, thermal decomposition, and electrochemical preparation, all of which can be combined with various nanotechnologies to achieve unique microstructures and advanced performances[59].

Here We must concentrate on transition metal oxides in this case due to their high performances.

## CV – Curve:

Cyclic voltammetry is an electrochemical technique for measuring the current response of a redox active solution with potential sweep between two or more set values. The cyclic voltammetry (CV) curve of EDLC supposed to be rectangular, but in pseudo-capacitance, the shape of the curve will become non-rectangular due to faradaic process. Hence, overall shape of the CV curve in hybrid type capacitors is a nonrectangular as it is combination of both EDLC and Pseudocapacitors.

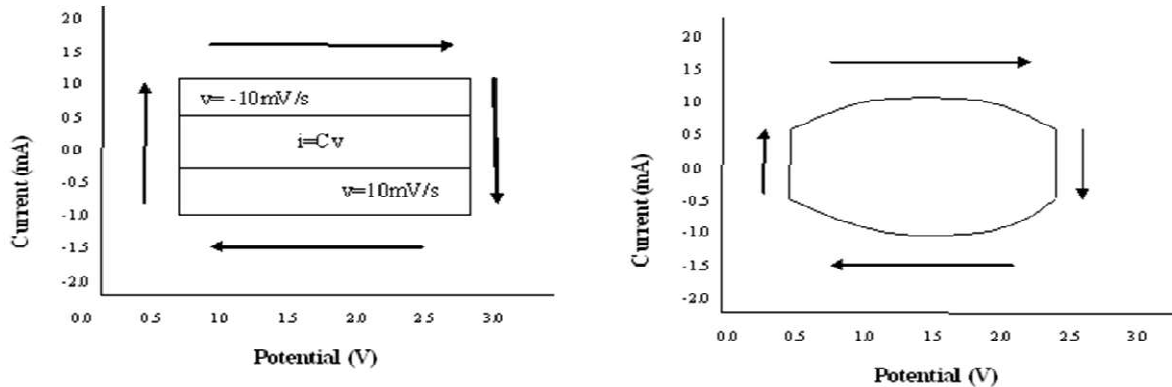


Fig 7 - Typical CV curve of EDLC and Pseudocapacitors

There are two major components of supercapacitor having some properties due to which it can store high capacitance energy, one is electrode and another is electrolyte.

## Transition metal oxides used as electrode materials :

### Ruthenium oxides :

There are two different phases of Crystalline ruthenium oxides i.e. rutile phase  $\text{RuO}_2$  and hydrated  $\text{RuO}_2 \cdot x\text{H}_2\text{O}$ . Ruthenium oxide is electrochemically stable in both crystalline and hydrous states. Buzzanca et al. in 1971 [60] showed hydrous  $\text{RuO}_2$  as a pseudocapacitive electrode material in an acidic supercapacitor electrolyte for the first time. Ruthenium is a rare earth metal that is 100 times more costly than manganese and nickel. We chose Ruthenium oxides as an electrode material for SCs because of its high conductivity, strong thermal stability, superior electrical conductivity, higher rate capability, and high specific capacitance of 750–2000  $\text{F g}^{-1}$  [61,62]. In an aqueous electrolyte, this capacitance is sufficient for the transition from  $\text{Ru(II)}$  to  $\text{Ru(VI)}$ . [63-64].

As Ruthenium is expensive and less available in earth crust, to overcome this problem researchers direct some alternative methods by which we can get more productive and high yielding of  $\text{RuO}_2$ .

Table- 1 ( preparation methods and specific capacitances )

No.	Prep. method	Film prop.	Sp. capacitance (F g <sup>-1</sup> )	Ref.
1	Hydrothermal	Hydrous RuO <sub>2</sub> with multi-walled carbon nanotubes (MWCNT)	1585	(Chaitra et al., 2016)
2	Facile template method	Hydrous RuO <sub>2</sub> nanotubes	746	(X. Wu et al., 2015)
3	- hydrothermal	1D RuO <sub>2</sub> □ 1.84 H <sub>2</sub> O	511	(Kim et al., 2015)
4	Laser scribing method	Graphene/RuO <sub>2</sub> nanocomposite	1139	(Hwang et al., 2015)
5	Hydrothermal	RuO <sub>2</sub> /graphene	29	(p.Leng et al., 2015)
6	Solution phase	RuO <sub>2</sub> /graphene	480	(S.Deng et al., 2014a)
7	ionic layer adsorption and reaction	PANI-RuO <sub>2</sub>	664	(Deshmukh et al., 2014)
8	Hydrothermal	RuO <sub>2</sub> -reduced graphene oxide (RGO)	521	(Shen et al., 2013)
9	Electropolymerisation and redox deposition	Nanoscopical RuO <sub>2</sub> /es	532	(D.Q. Zhao et al., 2012)
10	Chemical bath deposition (CBD)	RuO <sub>2</sub> thin film	73	(Patil et al., 2011)
11	Laser printing	SWCNT/RuO <sub>2</sub> nanowire	138	(P. Chen et al., 2010)
12	Sol-gel and low temperature annealing	Hydrous RuO <sub>2</sub> /graphene with particle-attached layered structure	570	(Z. ZHANG.-S. Wu et al., 2010)

. Several studies shows that by combining Ruthenium with other materials to form composite electrodes so that we can make the variety of ruthenium oxides composites and solve the cost excessive problem of ruthenium.

### Ruthenium oxide-based composites:

For example, a Ru–V–O composite containing RuO<sub>2</sub> and other oxides such as VO<sub>x</sub>, TiO<sub>2</sub>, MoO<sub>3</sub>, NiO/RuO<sub>2</sub>, SnO<sub>2</sub> and CaO, RuO<sub>2</sub>/PANi, PPy, carbon/hydrous RuO<sub>2</sub>, and others has a maximum capacitance of 290 F/g. Electrochemically generated RuO<sub>2</sub> is deposited on Ni, Ti, Pt, and Si foils through cathodicgalvanostatic deposition Literature reports that CVs of RuO<sub>2</sub>/TiO<sub>2</sub> electrodes are pseudocapacitive in behaviour. The RuO<sub>2</sub> based composite electrodes exhibit mixed capacitive behaviour in 1 M KOH, with a broad potential window of 0 to 1.4 V and an excellent SC of 120 F/g. The RuO<sub>2</sub>/TiO<sub>2</sub> composite electrodes produced have a low internal resistance of 1.5.Ω[65-68].

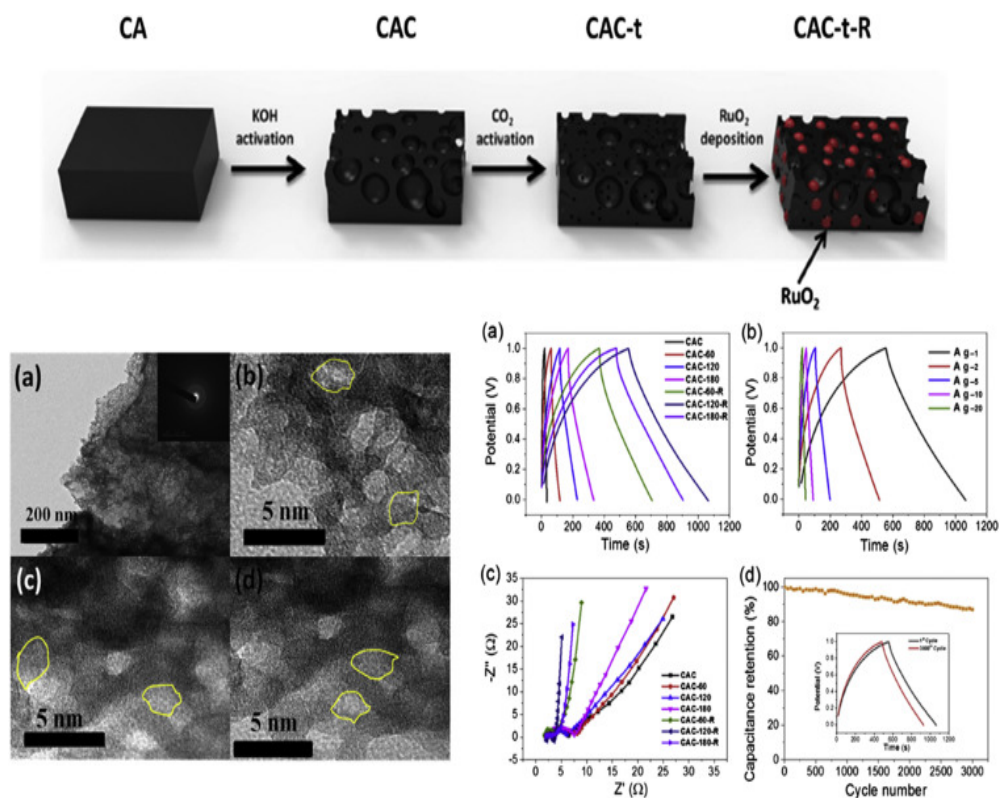
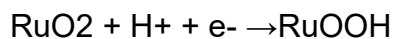


Fig 8 - schematic diagram and cv curve of RuO<sub>2</sub>-carbon composites

The energy storage mechanism of RuO<sub>2</sub> can be described in the equation as given below



or



The specific capacitance of anhydrous RuO<sub>2</sub> is 24 F/g over a large range of voltage (2.0 V), but hydrous RuO<sub>2</sub>·6H<sub>2</sub>O has a higher sp.Cap. of 343 F/g, as seen by the CV curve. As a result, hydrated RuO<sub>2</sub> has a greater specific

capacitance than anhydrous Ruthenium Oxides Amorphous Ruthenium Oxides has a greater specific capacitance of 1581 Farad per gram when compared to crystalline Ruthenium Oxides. because the amorphous structure's flexibility allows for solid structure depending on ion intraction, resulting in more active redox reaction sites [69-76]

Four variables have been postulated to determine the capacitance performance of RuO<sub>2</sub>.xH<sub>2</sub>O:

- (i) Electron hopping within RuO<sub>2</sub> .xH<sub>2</sub>O NPs;
- (ii) Electron hopping among RuO<sub>2</sub>. xH<sub>2</sub>O NPs and carbon particulates;
- (iii) Electron hopping between electrode materials and current collectors;and
- (iv) Proton diffusion with in RuO<sub>2</sub> .xH<sub>2</sub>O NPs

The capacitive properties of RuO<sub>2</sub>.xH<sub>2</sub>O are unaffected by NaAcO concentration or plating temperature, although the rate of deposition is affected by electrode shape and deposit adherence. The specific capacitance of RuO<sub>2</sub>. xH<sub>2</sub>O is linearly lowered from approx. Based on adhesion properties, capacitive performances, and deposition rate, RuO<sub>2</sub>.xH<sub>2</sub>O/Ti electrodes with RuO<sub>2</sub>.xH<sub>2</sub>O mass loading of 0.6mgcm<sup>2</sup> and annealing in air at 200 °c for 2h, plated from the 10mM RuCl<sub>3</sub>.xH<sub>2</sub>O solution with 10mM NaAcO around 50 °c should be the best choices for high-power applications.

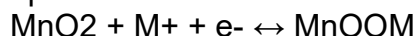
,Ruthenium oxide-based super- capacitors are commercially available in Taiwan as shown in the picture below



Fig9-Commercial SCmade up of RuO<sub>2</sub>- electrodes

### Manganese oxides:

Manganese (Mn) is a mineral found in nature in enormous amounts. Two types are ore and metal nodules. The cathodes used for the aqueous asymmetrical super capacitor devices were extensively investigated with manganese oxide materials. The transition metal oxide of manganese oxide is seven-stage oxidation: Mn(0), to Mn (VII). The discussion will take place on two of them. (MnO<sub>2</sub> and Mn<sub>3</sub>O<sub>4</sub>) are ecologically friendly and abundant on the globe and have a great operating potential window, a high special capacitance. Manganese oxide (MnO<sub>2</sub>) is cheaper and less harmful than ruthenium oxide-based supercapacitors. [77,78]The pseudocapacitive behaviour of Lee and Goodenough was suggested in 1999. With the following eqn may be defined the charging store in the supercapacitor:



Where  $M^+$  presents the alkali cations ( $Li^+$ ,  $Na^+$ ,  $K^+$ ).

Manganese oxide minerals are available in a variety of crystalline form, including  $\alpha$ ,  $\beta$ ,  $\gamma$ , and  $\delta$ , as depicted in Figure 10. These crystal forms can influence the pseudo capacitance of  $MnO_2$  electrodes. They include 1 Dimensional structures in a tunnel, 2 Dimensional layer and 3 Dimensional spinel. Due to its porous structure, electrolyte ions may be moved more rapidly, which results in a higher specific capacitance.  $K^+$ ,  $Li^+$  -Manganese oxide with a channel diameter of 4.61, and interlayer spacing of 7.1 is easily accommodated with an ionic diameter of 3.0 But manganese oxides and  $\mu$  are unable for transportation of  $K^+$  through a narrow channel (3.2).

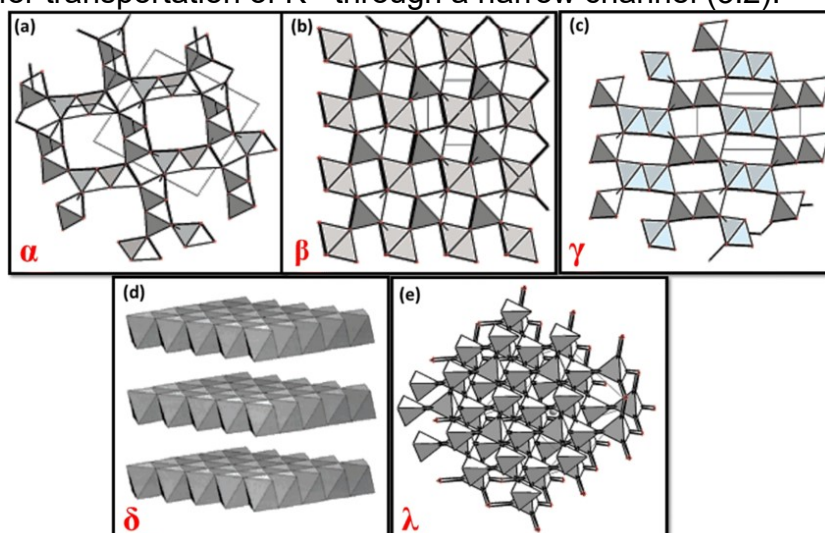


Figure 10 Alpha, beta, gamma, delta, lambda. Oxides of manganese

Some of the inconvenience of  $MnO_2$ -based electrode materials, which can restrict electron transportation, cycle-life and a particular surface area, include low electroconductivity and high dissolubility of basic and neutral electrolytes. We must dop  $MnO_2$  materials to improve their electrical conductivity. For example,  $Li_{1-x}Mn_xRu_xO_2$ , has a pseudo-capacitive property at 361 Farad per gramme. In order to increase the conductivity of  $MnO_2$  products, we use carbon materials such as active carbon, CNT, and graphite as well as polymers. Leading polymers are used as protective shells to avoid evaporation throughout the cycle of  $MnO_2$  compounds. The form of the  $MnO_2$  material plays a significant role in the achievement of high capacity and the surface area in terms of supercapacitor capacitance. Depending on their morphologies,  $MnO_2$  – specific areas of materials may cover from 20 to 306.9  $m^2 g^{-1}$ . The manganese oxides are therefore categorised as (0D), (1D), (2D) & (3D). [82-86]

SCs containing nanoparticles based on  $MnO_2$  0D were discovered..  $MnO_2$  painting techniques on 3-dimestic graphite-style capsules, as provided in Figure-11, were proposed by Jian et al. Jian. [87]  $MnO_2$  0D hollow structures have been literature extensively.. The special area of the  $MnO_2$  nanospheres reached by 253  $m^2 g^{-1}$ . This hollow structure also has a capacitance of 300 Farad per gramme at 6  $mV s^{-1}$ . [88]

The core-shell zero-dimensional nanostructures form a strong, hollow and thin shell. The nanostructures Core Shell 0D have a wide range of advantages such as huge specific surface areas, superior conductivity, high scatterability and chemical and

mechanical stability. Nanostructures constructed from C-MnO<sub>2</sub> have been produced from core shell. [89,90]

The many structures in 1D-MnO<sub>2</sub> nanostructures include nanorod, nanotubes and nanotubes. As demonstrated in Figure 11b, the hydrogenation approach for the production of oxygen-deficient MnO<sub>2</sub> nanorods providing 449 F g<sup>-1</sup> high speed capacity at 0.75 mA cm<sup>-2</sup>. MnO<sub>2</sub> performs extensively due to the concentration of oxygen vacancy (Figure 11c,d). This may cause electrochemical activity through changes in oxygen vacancy concentrations. Yao et al. were able to manufacture extremely long, 105 length-diameter MnO<sub>2</sub> nanowires by use of hydrothermal techniques.. MnO<sub>2</sub> nanotub arrays were produced in 10 minutes using anodic aluminium oxide (AAO) model, whereas MnO<sub>2</sub> nanotube arrays required 60 minutes. The MnO<sub>2</sub> Micro Tubes arrays have 320 F g<sup>-1</sup> capacity, whereas the MnO<sub>2</sub> nano Tubes have just 101 F g<sup>-1</sup> capacity. [91-93].

Due to the enormous specific surface surfaces and numerous active sites, were widely investigated. 2D nanostructuring may be utilised to produce electrodes that are stand-by and not require a substratum, in contrast to 0D and 1D nanostructures. A nanofilm with a high speed of 640.8 F g<sup>-1</sup> at 10 A g<sup>-1</sup> was produced on the active paper using the electrodeposition technique. MnO<sub>2</sub> nanofilms are often synthesised by the method of redox deposition. Hydrothermal 2D MnO<sub>2</sub> nanofilms have less mass burden than electrodeposition or redox repositioning films when it is a question of mass loading. A high specific conversion of 1035 F g<sup>-1</sup> at 2mV S<sup>-1</sup> may be achieved with a loading of 0.09 mg cm<sup>-2</sup> on 2D MnO<sub>2</sub> nanofilms (Mn paper-80) (Figure 11f)..Wang et al. have devised a sacrificial template approach for the production of MnO<sub>2</sub> nanosheets. [94.95].

.3Dimentional MnO<sub>2</sub> gives pathways to the electrolyte and provide a high S.A and stability of mechanical for SC electrodes. Bag et al. created the self-branche 3D-MnO<sub>2</sub>@-MnO<sub>2</sub>, a template-free approach (Figure 11g,h). With a wide specific area of 238 m<sup>2</sup>g<sup>-1</sup>, and a pore area of 3.6 nm, this 3D self-connected -MnO<sub>2</sub>@-MnO<sub>2</sub>, allows quicker transfer of loads. Zhu et coll have produced a novel 3D MnO<sub>2</sub> nanostructure consisting of nanoflocks -MnO<sub>2</sub> and -MnO<sub>2</sub>. [96.97].

Another Manganese oxide that is used as an electrode material is the Mn<sub>3</sub>O<sub>4</sub>, a Manganese oxide with an electrodestructure that provides a strong crystalline architecture with 3D diffusion channels. In comparison with MnO<sub>2</sub>, and Mn<sub>3</sub>O<sub>4</sub> has less electronic conductivity, with less capacities. Unknown is the process of Mn<sub>3</sub>O<sub>4</sub> energy storage. Recent investigations have been performed in situ X-ray absorption near-edge spectrum (XANES). [98,99]

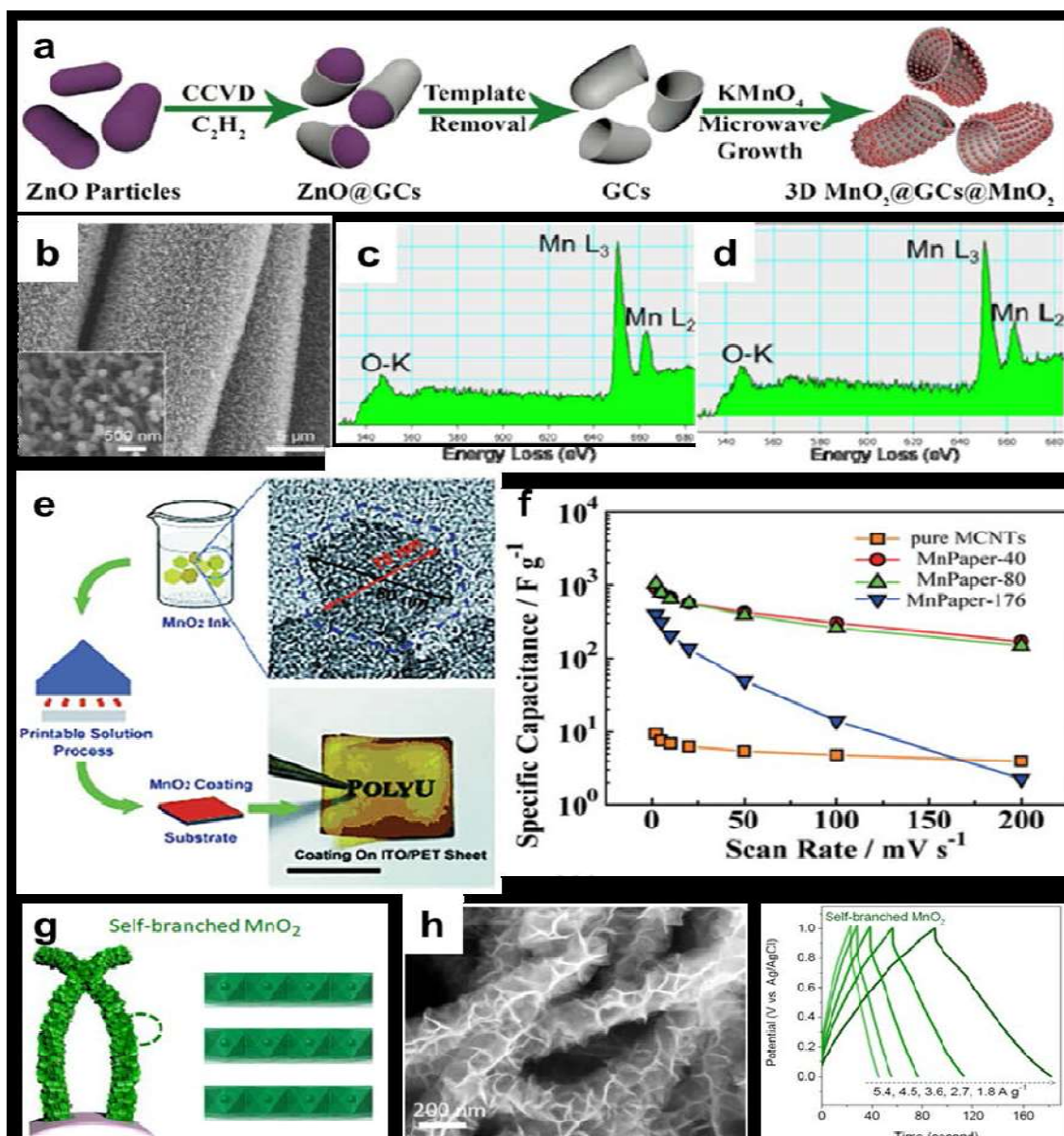


Figure 11.(a) synthesis of  $\text{MnO}_2@\text{GCs}@\text{MnO}_2$ . (b) FE-SEM image of  $\text{MnO}_2$  (c) edged part and (d)  $\text{MnO}_2$  NANOWIRES (e) TEM image of  $\text{MnO}_2$  (f) specific capacitance with scan rate for 2D  $\text{MnO}_2$  (g) branched  $\text{MnO}_2$  electrode (h) FE-SEM image, and (i) GCD curves .

The Porous Nanoparticles  $\text{Mn}_3\text{O}_4$  (NPs) with the synthesis of tube (F127) as a dispersant in fig. 12. Porous nanoparticles (NPs). The amorphous manganese precursors should be uniformly dispersed onto the polymer due to the affinity of the  $\text{Mn(II)}$  ion of the hydrophilic part of F127. [100]

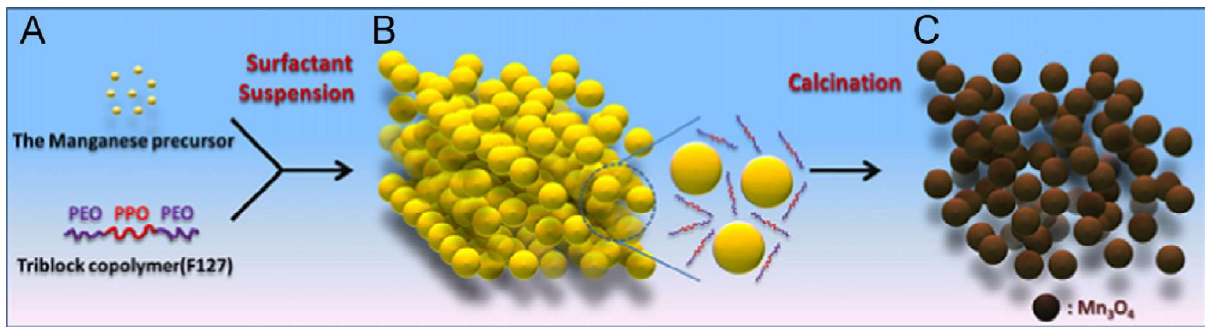


Fig.12.The thermal decomposition strategy of nanocrystals  $Mn_3O_4$ ; Step(A): manganese acetate and copolymer triblock was dissolved into the methanol; Step(B): suspension of copolymer triblock and phase-transformation manganese acetate; Step(C):  $Mn_3O_4$  nanoparticles formed under calcination.

Zhou et al. also established a straight forward synthesising technique, as shown in Fig. 13, for freestanding  $MnO_2$ -nanoplates/Porous Carbon Fibres (PCNFs) ( $MnO_2$ /PCNFs). The  $MnO_2$  nanoplates are vertical on the outside surface of the PCNF, which contribute to a considerable area between the PCNFs, as seen by electron microscopy (SEM) scanning pictures. A significant degree of mesoporosity and a big area (1814  $m^2/g$ ) were present in the  $MnO_2$ /PCNF produced and 92,3 percent of the initial capacitance was preserved after 4,000 cycles. However, compared to  $MnO_2$ /PCNF it was found that the results of Electrochemical Spectroscopy (EIS), which was attributed in great part to the very high conductivity of the el [101-103], showed that PCNF had a lower impedance to charge transmission.

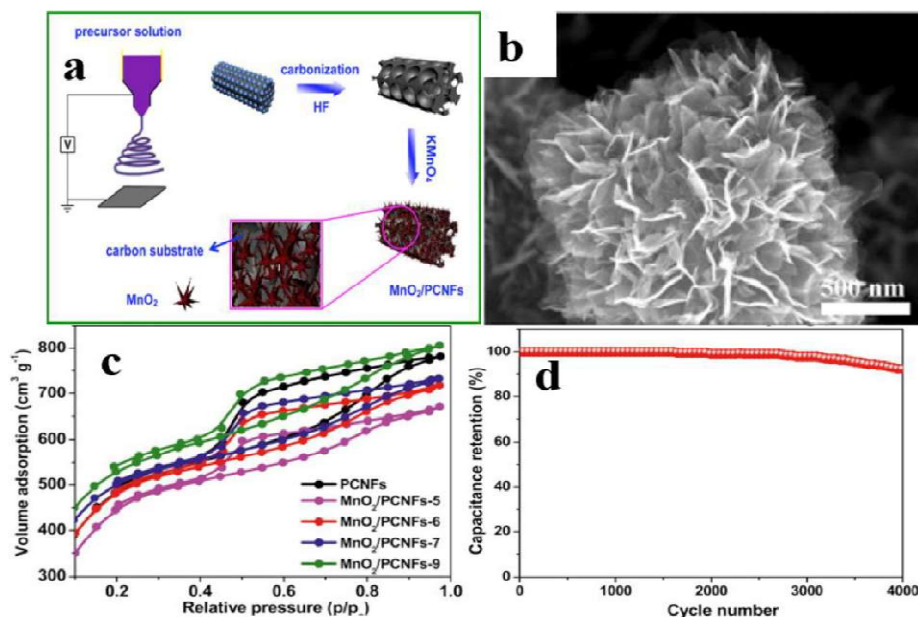


Fig. 13(a)  $MnO_2$ /PCNF synthesis schematic depiction.

(b)  $MnO_2$ /PCNFs-6 SEM picture.

(c) PCNF and  $MnO_2$ /PCNFs with differing weight ratios of  $KMnO_4$  and PCNFs adsorption/desorption isotherms in nitrogen.

(d)  $MnO_2$ /PCNFs-6 electrode long-term stability with a current density of over 4000 cycles of 0,5 A/g.

Table 2 (The film properties with specific capacitance of MnO<sub>2</sub>)

No.	Prep. method	Film prop.	Sp.Cap.(Farad per gram)	Reference
1	Anode depo.	MnO <sub>2</sub> nanostructure on gold film	432	(Shi et al., 2017)
2	Electrodeposition	Co <sub>3</sub> O <sub>4</sub> □MnO <sub>2</sub> □NiO nanotubes	2526	(A.Singh et al., 2016)
3	pyrolysis	Mn <sub>3</sub> O <sub>4</sub> thin film	395	(BB.Yadav et al., 2016)
4	Hydrolysis of Urea	NiMnO <sub>2</sub> layered double hydroxide	1512	(Guo et al., 2016)
5	Electrodeposition	CoMnO <sub>2</sub> layered double hydroxide	1063	(Jagadale et al., 2017)
6	reaction of Sacrificial	Manganese oxide decorated graphene sheets	280	(Unnikrishnan et al., 2016)
7	Anodic deposition	Mn-Ni oxide	251	(Tahi et al., 2016)
8	S-gel method	Manganese oxide (MWCNT)	335	(S.-H. Cheen et al., 2016)
9	S-gel method	MnO <sub>2</sub> oxide film	361	(Sark.et al., 2015)
10	Hydrothermal	Mn <sub>3</sub> O <sub>4</sub> /graphene	367	(H.-M. Lee et al., 2015)
11	Hydrothermal	Ni(OH) <sub>2</sub> /MnO <sub>2</sub> /RGO	1985	(H. Chen et al., 2014)
12	Electrospinning	/MnO <sub>2</sub> core-shell tubular structure	237	(Hon.g et al., 2014)
13	Electrospinning	Carbon nanofiber/MnO <sub>2</sub>	311	(Zhi et al., 2012)
14	Hydrothermal	NiMnO <sub>2</sub>	284	(C.-H. Wu et al., 2012)
15	Cat. deposition	Manganese oxide thin	365	(Liu et al., 2010)

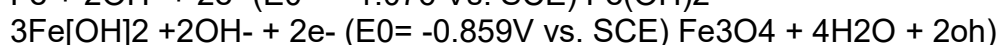
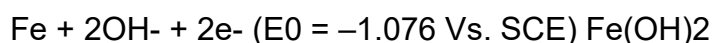
It is important to note that in thin films, MnOx works better. Since on the ground only there is a light coating of snow. In addition, during cycling, thick layer greatly reduces electrochemical performance. In contrast to patla film, the thin film offers a superior layer on the substratum that lowers the ion transportation barrier. The substrate used impacts the electrochemical performance significantly. By employing a conduction network, the capacity may be enhanced. The carbon substance is the most common fault in the conduction network. The proper usage of carbon material like MWCNT contributes to the construction and maintenance of porous structures and network relationships.

MnOx can also be mixed with an excellent carbon compound called graphene. MnOx particles attached to the graphene sheets do not stack graphene sheets, whereas graphene sheets do not cluster MnOx particles. There are a lot of additional things to consider in addition to carbon monoxide. Nickel was included and the particle size was changed from rod-like to plate-like.. The ternary composite is also widely investigated. Ternary hybrid nanotubes have exhibited excellent electrical performance via Co3O4-MnO2-NiO (2525 F g-1). It is because of the sophisticated arrays of nanotubes, which can readily permeate the electrolytes. The hydrothermal Ni(OH)2/MnO2/RGO generated on the other hand has a particular 1985 F-1 capacitance. The development of a porous floral structure has helped to store the load. [104-114]

## Iron oxides:

The, broad working fencing with -ve potential, non-toxic, earth-abundant, less costhigh theoretical capacity, environmental friendly, low ESR material, Amorphous and monocrystalline material with pseudo-Capacitors and other benefits are commonly used as an electrodes for Supercapacitors such as Fe2O3 and Fe3O4. Ma has studied iron oxides' energy storage methods to understand better how they store energy [115-118].

The oxidation processes of Fe3O4 may be described as below



One putative feed storage method of FeOx appears in the neutral aqueous electrolytes in the equation as  $\text{FeOx} + z\text{M}^{++} + y\text{e}^-$  or  $\text{MzFeOx}$

Where M is Li, Na, or K.. [119]

A potential anode material between two iron oxides is porous Fe2O3. Fe2O3 has a structural, optical, electrical and physical effect on its concentration. The characteristics of semi-conducting may be shown with iron oxide. Fe (III) is a semiconductor of n-type, while Fe (II) is a highly-doped, narrow band divider of the p-type semiconductor and so on. On t, the largest transitions in Fe redox Iron oxide is an effective oxidising agent to improve SC and conductivity while reducing ESR for Polymer Composites, inorganic, non-metallic composites and supercapacitor electrodes.

SC findings for an iron oxide-based electrode are good with a moderated potential window. The resistance of the electrode build up in the electrochemical series is low.

Fe<sub>2</sub>O<sub>3</sub> materials' crystal morphologies are essential to electrochemical performance modifications.

Figure 14 sums together four distinct crystal structures, including (Hexagonal structure centred in the Rhinos), (CBC), (CUBS), and -Fe<sub>2</sub>O<sub>3</sub> Figure 14 (orthorhombic structure). When compared with other crystal structures, -Fe<sub>2</sub>O<sub>3</sub> has a unique form, which makes it a good electrode material for long lasting SCs and has a greater thermodynamic stability. Other intermediate phases, including -Fe<sub>2</sub>O<sub>3</sub>, can be produced by heat treatment to -Fe<sub>2</sub>O<sub>3</sub>. [120,121]

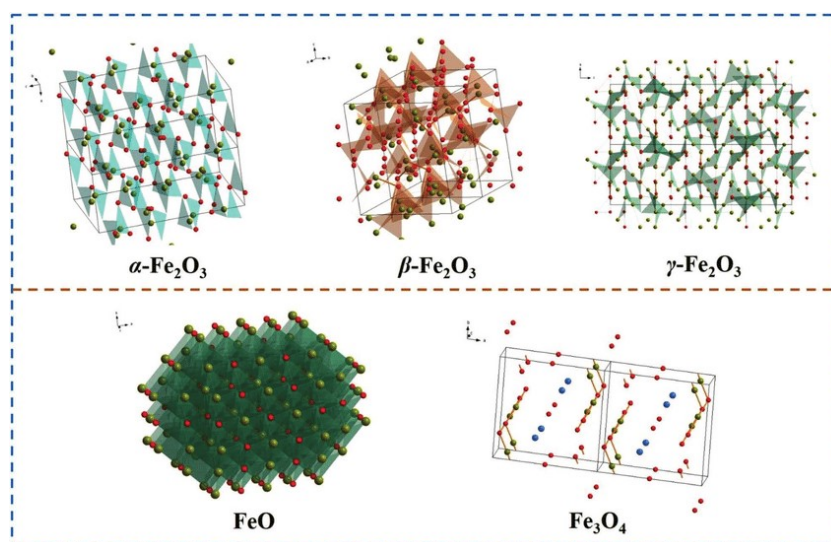


Figure 14.  $\alpha$ ,  $\beta$ ,  $\gamma$ ,  $\delta$ -Fe<sub>2</sub>O<sub>3</sub>, and Fe<sub>3</sub>O<sub>4</sub> crystallines. Figure 14. Reproduced by licence (Xia et al. 2016). 2016, Wiley, Copyright.

A range of variables, including crystal structures, morphology and compositions, impact the electrochemical properties of iron oxides. Many approaches were presented to enhance the specific capacity, cycle stability and specified iron oxide rate capacity in light of the factors, including the nanostructure engineering and the hybridisation components. The application of methods for nanostructural engineering can enhance survival.

Various approaches have recently been developed for the manufacture of Fe<sub>2</sub>O<sub>3</sub> nanostructures from 0D to 3D,..[122-124].

In general, 0D nanostructures are spherical nanoparticles. For example, Shivakumara et al. utilised sol-gel to produce -Fe<sub>2</sub>O<sub>3</sub> solid nanoparticles with an enormous specific area of 386 m<sup>2</sup> g<sup>-1</sup> (Figure 15a,b). The generated nanoparticles – Fe<sub>2</sub>O<sub>3</sub> (Nano Fe<sub>2</sub>O<sub>3</sub>) had a specific capacitor of 300 F-g<sup>-1</sup> in 1 A g<sup>-1</sup> on an electrolyte 0.5 M Na<sub>2</sub>SO<sub>3</sub>. [125]

The 1D nanostructures of Fe<sub>2</sub>O<sub>3</sub>, such as nanodes, nanowires and nanotubes, are used as electrode materials because they are extremely special surfaces, have a great 1D electron transport pathway and have a lot of flexibility in ion intercalation. Lu et al. employed techniques of thermal and solvothermal disintegration to create 1D-Fe<sub>2</sub>O<sub>3</sub> nanorods in a flexible carbon fabric (Figure 15d) which are oxygen deficient (N-Fe<sub>2</sub>O<sub>3</sub>). Superior capacitance of the oxygen-deficient nanorods -Fe<sub>2</sub>O<sub>3</sub> (N-Fe<sub>2</sub>O<sub>3</sub>) was 382.7 mF cm<sup>-2</sup> compared with oxygen-rich -Fe<sub>2</sub>O<sub>3</sub> nanorods., at 0.5 mA cm<sup>-2</sup> in a watery electrolyte of 3 M LiCl as contrasted with the -Fe<sub>2</sub>O<sub>3</sub> vacancy free of oxygen (A-Fe<sub>2</sub>O<sub>3</sub>) (Figure 15e). A combination solvothermal

decomposition technique has been employed for the manufacture of Fe<sub>2</sub>O<sub>3</sub> nanowires. Fe<sub>2</sub>O<sub>3</sub> has a high conductivity of nanowires .[126]

2D nanostructures enhance the electrolyte contact surface while minimising the ion diffusion pathways and enhancing capacitive performance. As demonstrated in Figure 15g, Liu et al employed an electrochemical induced technological method to produce ultrathin  $\alpha$ -Fe<sub>2</sub>O<sub>3</sub> nanoflakes of  $\alpha$ -Fe<sub>2</sub>O<sub>3</sub> nanorods. A higher areal capacitance at 1 mA cm<sup>2</sup> (Figure 15h) than the  $\alpha$ -Fe<sub>2</sub>O<sub>3</sub> Nanorods-based Electrode (NR), due to its enhanced surface surface and reduced resistance, generated the obtained nanoflake electrode (NF) of  $\alpha$ -Fe<sub>2</sub>O<sub>3</sub> (Figure 15i). [127,128].

Zheng et al. employed a hydrothermal method for producing 3D -Fe<sub>2</sub>O<sub>3</sub> hollow, 30 nm wall thick holes and 100 nm length nanoshuttles (Figure 15j). The nanoshuttle hollow -Fe<sub>2</sub>O<sub>3</sub> has a high capacity as Figure 15k shows. s demonstrated in Figure 15l, the special capacitance of hollow nanoshuttles -Fe<sub>2</sub>O<sub>3</sub> has changing from 20° C (203 F g<sup>-1</sup>) to 60° C, little (234 F g<sup>-1</sup>). [129]

For SCs with various morphologies another common iron oxide, Fe<sub>3</sub>O<sub>4</sub>, was generated and studied. For the formation of Fe<sub>3</sub>O<sub>4</sub> nanoparticles, the Fe<sup>2+</sup>/Fe<sup>3+</sup> molar ratio should be 0.5. But the Fe<sub>3</sub>O<sub>4</sub> nanoparticles are easily combined, leading to large particles with a little surface area. Wang et al. utilised an ultrasonic aided technique for producing Fe<sub>3</sub>O<sub>4</sub> 2 m diameter nanoparticles. [130-133]

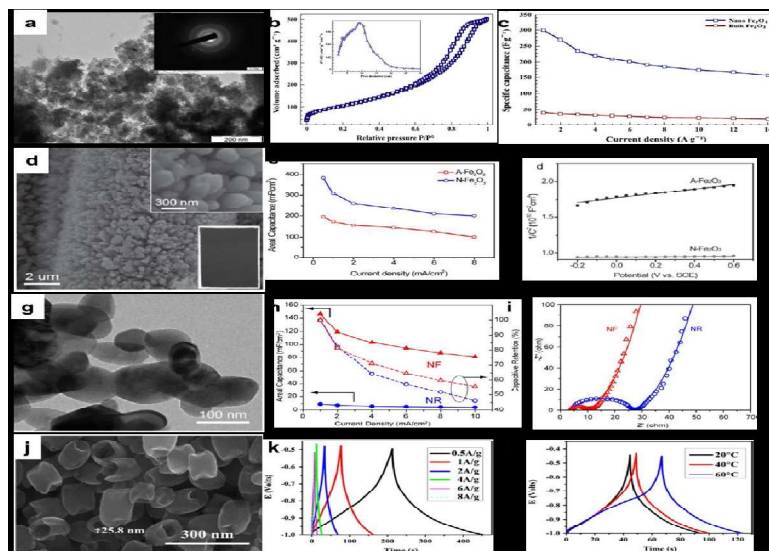


Illustration 15.(a) SEM IMAG (b) N<sub>2</sub> adsorption-desorption isotherm and (c) Fe<sub>2</sub>O<sub>3</sub> nanoparticle rate capability. (d) picture-FE-SEMs, (e) capacity rates, and (f) pplots of  $\alpha$ -Fe<sub>2</sub>O<sub>3</sub> (g) TEM plots, (h) capacity rates (I) curves of GCD (j) FE-SEM picture, (k) GCD curves of various current densities,

## Nickel oxides:

Because of their huge surface area, its high pseudo-capacity and its low cost, Ni(OH)<sub>2</sub> has been widely studied in transition metal oxides. Nickel and nickel oxide are commonly employed in rechargeable batteries and supercapacitors because of their low toxicity and comparable electrochemical conduct. This electrode is essential in the manufacture of supercapacitors because of its ionic characteristics. The greatest value of SC 703 F/g was obtained for the flower-species with a wide surface area in 6-M KOH electrolytes at potential windows of 0 to 0.5 V at a 2 mV/s scan rate. The high surface porosity structure significantly improves the transfer of charge and capacity of an electrode. The two dimensional (2D) and three-dimensional (3D) nano arrays display outstanding electrical capabilities due to their large volume surface, good structure and open form. NiO was generated in many morphologies including nanoparticles, nanoparticles, nanoparticles and nanosheet-based NiO-sphere-sphere, nanoparticles, nanofibers, nanosheets, nanotubes, architectures of flowers and hollow spheres. The CV curve shape shows a SC value and a restricted window for redox pinnacles. The resistance of the built electrode to electrical chemicals is low. The Co (OH)<sub>2</sub>/Ni composite electrode works effectively with a large potential window of 0.1 V to 0.6 V and high SCs of 1017 F/g in 2 M KOH. [134-149]

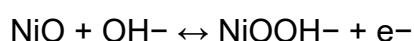
Table -3 (synthesis settings for nickel oxide/hydroxide deposition details and thin films of their composition using electrodeposition method) (Ref.-S.G.Sayyed, et.al 2019)

Sno	Chemical /Bath Composition & conditions	Substrate Electrode		Details						Remarks/Properties	SC
		A	K	R	APP . VOL T.	DEP O. TIME	TE M.	SCAN RATE	ELECTROL YTE		
1	0.08 M Ni(NO <sub>3</sub> ) <sub>2</sub> , After deposition film was thermal treated at in air at 250°C (temp rate: 5 °C/min)	Ni	P t	SCE	- 0.90	-		40	1M KOH	Formation of α - nickel hydroxides with the grain size of 3.48 nm. The capacitance maintained up to 87% of maximum capacity after	1478

	in muffle stove for 2 h.									500 cycles	
2	0.13M sodium acetate + 0.13M nickel sulfate + 0.1M sodium sulfate. After deposition film was dried at 300°C in air for 1 h.	SS	Pt	Ag-AgCl	0.5 mA/cm	60MIN	Room temperature	25	1M KOH	Film exhibits highly porous morphology with nanoflakes like structure of thickness 12–16 nm. XRD pattern indicates that the formation of NiO with poor crystallinity. 87.5% retention of capacitance after 5000 cycles.	167.3
3	Three solution: NiCl <sub>2</sub> ·6H <sub>2</sub> O (NiO-C), Ni(NO <sub>3</sub> ) <sub>2</sub> ·6H <sub>2</sub> O (NiO-N) and NiSO <sub>4</sub> ·6H <sub>2</sub> O (NiO-S), After deposition films were annealed in air at 500°C for 2 h.	SS	Gh	SCE	NiO-C: -0.75 to -0.6 V NiO-N: -0.7 to -0.55 V NiO-S: -0.8 to -0.65	30MIN	Room temperature	5	1M KOH	All electrodes showed the cubic phase of NiO. It was observed that the growth of nanoflakes uniformly distributed on the surface. NiO-S electrodes showed all over good performance i.e. high capacitance, low impedance 1.27Ω/cm <sup>2</sup> and high surface area 91.5 m <sup>2</sup> /g	893

										with better stability (85.6%).	
4	0.1 M Ni(NO <sub>3</sub> ) <sub>2</sub> , After deposition film were annealed at 573 K for 90 min.	SS	Gh	SCE	0 to -1.2 V at scan rate: 50mV/s	30cycles		100	1M KOH	Formed NiO nanoflakes thin film showed specific power of 1.0 kW/kg and energy 14.6Wh/kg. Impedance of prepared film was 1.34Ω and cyclic stability up to 94% over 1000 cycles	222
5	0.08 M Ni(NO <sub>3</sub> ) <sub>2</sub> ·6H <sub>2</sub> O	Ni	Pt	Ag-AgCl	- 0.90 V	-	Room temperature	-	1M KOH	α-Ni(OH) <sub>2</sub> showed particle like morphology with a loosely packed structure.	2595
6	3 mM Ni(NO <sub>3</sub> ) <sub>2</sub> ·6H <sub>2</sub> O + 3 mM Fe(NO <sub>3</sub> ) <sub>3</sub> ·9H <sub>2</sub> O	NF	Pt	Ag-AgCl	- 1.0 V	300s	10°C	5	1M KOH	The formation of interconnected mesoporous structures with the pore size of 50 nm.	

NiO redox reaction may be characterised as follows in an alkaline electrolyte:



The electrochemical performance of NiO is entirely caused by the crystallinity which is altered by heat treatment. Wu et al. found that nickel hydroxide was transformed to nickel oxide with a high SC of 1478 by nickel hydroxide placed on Nickel substrate at 250 degrees Celsius. The sulphate solution NiO Electrode has good electrochemical characteristics in all areas.

However, two significant drawbacks are the use of NiO for supercapacitor electrode I which has low cycle stability. (ii) poor conductivity electricity. In order to avoid these inconveniences, it is recommended to compose NiO with other substances and produce nanostructured NiOs

In addition, the binary oxide of NiCo<sub>2</sub>O<sub>4</sub> has shown its outstanding electrochemical efficiency that has international attention. This can be done in a straightforward way, such as co-precipitation or hydrolysis. The co-precipitation technology resulted in a 1211 F g<sup>-1</sup> compound of NiCo<sub>2</sub>O<sub>4</sub>/graphene oxide.

Sodium dodecyl Sulphate Morphology for NiCo<sub>2</sub>O was investigated (SDS).. NiCo<sub>2</sub>O<sub>4</sub>/SWCNT, on the other hand, has a specific capacity of 1642 F g<sup>-1</sup> that uses a controlled hydrolysis method. The water:ethanol ratio has been adjusted to identify the optimal solvent composition of NiCo<sub>2</sub>O<sub>4</sub>/SWCNT electrode. Different ratios of water and ethanol result in different morphologies. A 1:4 ratio of water to ethanol was discovered to be the optimal condition for electrode production. [150-154].

## NiMn<sub>2</sub>O<sub>4</sub> as supercapacitor applications

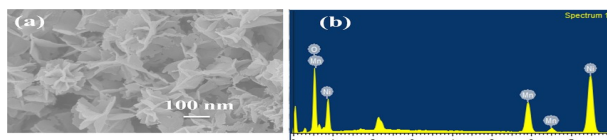
Because of their excellent electrical performance, NiMn<sub>2</sub>O<sub>4</sub>, a single phase spinel-structured product, has just become more prominent than many other metal oxides. For electrically powered materials and excellent electrochemical performance, high energy density and high energy densities are necessary when used as electrodes, as already mentioned. Due to its outstanding electrochemical performance, a single-phase spinel-structured NiMn<sub>2</sub>O<sub>4</sub>, is attracted much attention recently.

As has previously been said, high density and high density electrodes demand high conductivity materials and good electrochemical performance.

### Morphological characterisation

This FESEM image contains densely packaged NiMn<sub>2</sub>O<sub>4</sub> agglomerated nanoparticles 6 to 10 nm (8 nm mean size). The excess contact area of the material with the electrolyte efficiently generates a porous surface with a highly special surface area, thereby increasing electrochemical performance of electrodes, via the creation of densely packed small NiMn<sub>2</sub>O<sub>4</sub> nanoparticles. Surface area measurements using Brunauer-Emmett-Teller (BET) reveal NiMn<sub>2</sub>O<sub>4</sub> nanostructures' porous nature.

The typical type IV NiMn<sub>2</sub>O<sub>4</sub> isotherm, according to its mesoporous structure, appears in Figure 16. Figure 16. The material has a specified area of 43.6 and an average pore size of 13.3 nm, which implies that there are a lot of electrochemical locations involved..



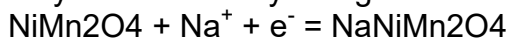
Nanoparticles SEM picture NiMn<sub>2</sub>O<sub>4</sub>



Figure 16: N<sub>2</sub> adsorption-desorption and pore size of NiMn<sub>2</sub>O<sub>4</sub>.

## Electrochemical characterization:

The CV curves of the NiMn<sub>2</sub>O<sub>4</sub> Electrode demonstrate Faradic charge transfer compoartamiento owing to functional group or poresize dispersion. The CV curves shows the redox nature of the electrode material and informs the electrode about its pseudocapacitive conduct. Several peaks in CV (Mn<sup>3+</sup>, Mn<sup>4+</sup> and Ni<sup>2+</sup> and Ni<sup>3+</sup>) may also be readily recognised because of the Eq-related faradic redox processes.



A scan rate of 2 mV s<sup>-1</sup> was obtained by measuring the specific capacitance (C<sub>m</sub>) of the electrode for each scan rate using the CV curves. The greatest specific capacitance was reached at 875 g 1. The diagrams demonstrate clearly a decrease in the loading/unload time of the increased density of the current, which may be explained by ion diffusion.

Na<sup>+</sup> ions from the electrolyte solution occupies a broad electrode surface at lower current densities as they have more time to approach the maximum active sites of the electrode and result in increased specific capacity.

[155,156]

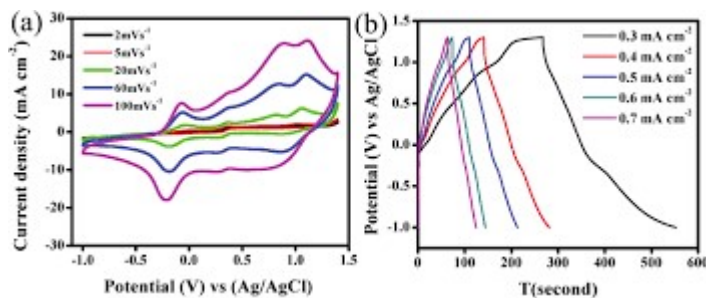


Fig -17(a) CV curves at various scans, and (b) GCD curves for the NiMn<sub>2</sub>O<sub>4</sub> composite at differing current densities.

## Other metal oxides :

All the materials used as supercapacitor, in addition to RuO, MnO, NiO and CoO, FeO electrodes were explored as copper oxide (CuO), Vanadium oxide (VO), Molybdenum oxide (MoO), Titanium oxide (TiO), Tin oxide (SnO), BiO, and Indium oxide (InO). The electrical deposition on several substrates of thin copper oxide

amorphous films such as copper oxide produced with copper foam was utilised to make copper oxide amorphous thin films. According to Ghadge et al, the copper hydroxide thin film electrode generated by anodizing method has a special capacitance of up to 6000 F/g. TiO has been coated using an electro-chemical anodization technique on titanium metal foil which results in 1300 F/cm<sup>2</sup> of specific capacity. The amorphous VO has a maximal specific capacity of 350 F per g, according to Lee et al. The amorphous, electrodepositionally manufactured MoOx sheet has a capacity of 507 F/g in a 1-M H<sub>2</sub>SO<sub>4</sub> solution. The thin layer on a copper substratum is 98 F/g for the particular capability of electrodepositing Bi<sub>2</sub>O<sub>3</sub>. Amorphous SnO generated by electrochemical deposition has the greatest specific capacity of 285 F/g. Prasad et al. developed In film with a specific capacitance of 190 fg [157-166], using the electrochemical deposition method. Due to their high theoretical capabilities from the faradaic load transfer mechanism, several TMOs are often used in supercapacitors including ruthenium oxide (RuO<sub>2</sub>), manganese oxide (MnO<sub>2</sub>), nickel oxide (NiO), cobalt oxide (CO<sub>3</sub>O<sub>4</sub>) and vanadium oxide (V<sub>2</sub>O<sub>5</sub>). [167-172]

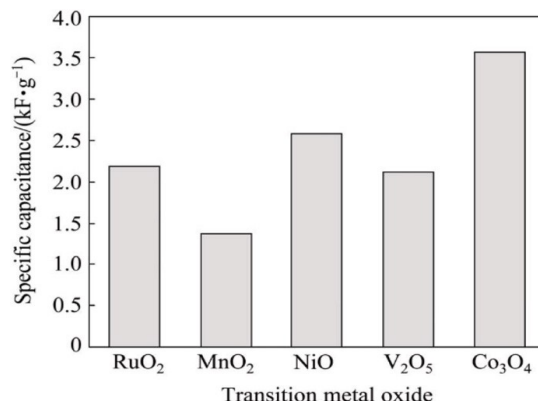


Fig-18 Comparison of several TMOs' putative particular capabilities

## CONCLUSION

Metal oxide appears like a viable electrode material for supercapacitor applications. Metal oxide based electrode electrodes have a variety of structures, created by distinct production methods, diverse material combinations and a number of experimental conditions that impact their electrochemical performance. Charge storage processes in different additives. With more knowledge of charge storage mechanism in different material combinations, the electrochemical performance of the supercapacitor electrode may be enhanced. Supercapacitors are a new form of energy storage device with higher energy density, excellent electrical properties and cyclical stability. In a broad rank, the smaller dielectric and higher thermal and electrochemical conductivity may be used in a range of applications including emergency energy sources, specialised power systems, ackup and pulse power. In addition, the creation of supercapacitors for electric car hybrid systems has proven quite interesting. Different transition metal oxides/hydroxides may be easily produced into supercapacitors due to their high conductivity, larger areas and improved stability. Metal oxide and hydroxide electrode supercapacitors and composite materials may achieve outstanding performance. The focus of research should be on generating new high capacity, high energy, high power and a greater variety of uses for electrodes.

## **REFERENCES---**

1. A.Roy, A.Ray, S.Saha, S.Saha, Transition metal oxide based nano materials for energy storage, 2018, 43, 1-2
2. A.Roy et al., Electrochemical Properties of TiO<sub>2</sub>-V<sub>2</sub>O<sub>5</sub> nano composites as a high performance supercapacitor electrode material. Applied Surface Science, 2018, 443, 581-591.
3. NASA, 2009, Second warmest year on record, End of warmest decades, 2010, Jan 21
4. S.G.Sayyed, M.A.Mahadik, A.V. Shaikh, J.S. Jang, and H.M.Pathan, 2019, 3, 25
5. R.C.Ambare, R.S.Mane and B.J.Lokhande, 2016, 4, 1943-1944
6. A.G.Pandolfo, A.F.Hollencamp, J of power sources, 2006, 27, 157
7. X.Andrieu, Energy storage system electron, New trends electrochemotechnol, 2000, 1, 521
8. K.Naoi, P.Simon, electrochem. Soc. Interface. (spring 2008), 38
9. S.G. Kandalkar, J. L. Gunjekar, C.D. Lokhande, ppl. Surf. Sci. 254, 5544 (2008).
10. T. Brousse, D. Bélanger, Electrochem. Solid-State Lett. 6, A248 (2003).
11. B.E. Conway, J. of Electrochem. Soc. 138, 1548 (1991).
12. J.P. Zheng, T.R. Jow, J. of Electrochem. Soc. 142, 6 (1995).
13. H. K. Kim, T. Y. Seong, J. H. Lim, Y. W. Ok, W. I. Cho, Y.H. Shin, Y.S. Yoon, J. Vac. Sci. Technol. B 20 (5), 1827 (2002).
14. Y.S. Yoon, W.I. Cho, J.H. Lim, D.J. Choi, J. of Power Sources, 101, 129 (2001).
15. C.An, Y.Zhang, H.guo, and Y.wang, Metal oxide based super capacitor – progress and prospective, 2019, 1, 4644-46
16. L. Huang, D. Chen, Y. Ding, S. Feng, Z. Wang and M. Liu, Nano Lett., 2013, 13, 3135–3139.
17. S. Chen, M. Xue, Y. Pan, L. Zhu and S. Qiu, J. Mater. Chem. A, 2015, 3, 20145–20152.
18. F. Wang, X. Wu, X. Yuan, Z. Liu, Y. Zhang, L. Fu, Y. Zhu, Q. Zhou, Y. Wu and W. Huang, Chem. Soc. Rev., 2017, 46, 6816–6854.
19. R. Salunkhe, Y. Kaneti and Y. Yamauchi, ACS Nano, 2017,

- 11, 5293–5308.
- 20.** L. Zhang, D. Shi, T. Liu, M. Jaroniec and J. Yu, *Mater. Today*, 2019, **25**, 35–65.
- 21.** Y. Dong, Y. Wang, Y. Xu, C. Chen, Y. Wang, L. Jiao and H. Yuan, *Electrochim. Acta*, 2017, **225**, 39–46.
- 22.** H. Kim, J. Cook, H. Lin, J. Ko, S. Tolbert, V. Ozolins and B. Dunn, *Nat. Mater.*, 2016, **16**, 454.
- 23.** M. D. Stoller, S. Park, Y. Zhu, J. An and R. S. Rouf, *Nano Lett.*, 2008, **8**, 3498.
- 24.** H. P. Wu, D. W. He, Y. S. Wang, M. Fu, Z. L. Liu, J. G. Wang and H. T. Wang, *IEEE*, 2010, 465.
- 25.** B. Rajagopalan and J. S. Chung, *Nanoscale Res. Lett.*, 2014, **9**, 1.
- 26.** C. D. Lokhande, D. P. Dubal and O. S. Joo, *Curr. Appl. Phys.*, 2011, **11**, 255–270.
- 27.** R. Kotz, M. Carlen, *Electrochim. Acta*, 2000, **45**, 2483–2498.
- 28.** P. Simon and Y. Gogotsi, *Nat. Mater.*, 2008, **7**.
- 29.** S. M. Chen, R. Ramachandran, V. Mani and R. Saraswathi, *Int. J. Electrochem. Sci.*, 2014, **9**, 4072 – 4085.
- 30.** A. Shukla, *Resonance*, 2001, **6 (8)**, 72–81.
- 31.** A. Schneuwly, R. Gallay, *Proceedings PCIM*, 2000, 1–10.
- 32.** C. Meng, O. Z. Gall and P. P. Irazoqui, *Biomed. Microdevices*, 2013, **15**, 973–983.
- 33.** X. Li and B. Wei, *Nano Energy*, 2013, **2**, 159
- 34.** L. L. Zhang, R. Zhou and X. S. Zhao, *J. Mater. Chem.*, 2010, **20**, 5983
- 35.** T. Chen, H. Peng, M. Durstock and L. Dai, *Sci. Rep.* 2014, **4**, 3612.
- 36.** Conway BE. *Electrochemical supercapacitors. Scientific Fundamentals and Technology Applications*. Ch 9; 1999
- 37.** Conway, B. E. (1999). *Electrochemical Supercapacitors: Scientific Fundamentals and Technological Applications*: Springer US.
- 38.** Roy A, Ray A, Saha S, Das S. Investigation on energy storage and conversion properties of multifunctional PANI-MWCNT composite. *International Journal of Hydrogen Energy*. 2018;43:7128-7139
- 39.** K. Chen, Y. Yang, K. Li, Z. Ma, Y. Zhou and D. Xue, *ACS Sustain. Chem. Eng.*, 2014, **2**, 440–444.
- 40.** R. Ramachandran, M. Saranya, V. Velmurugan, B. P. C. Ragupathy, S. K. Jeong and A. N. Grace, *Appl. Energy*, 2015, **153**, 22– 31.
- 41.** W. Chen, R. B. Rakhi and H. N. Alshareef, *J. Phys. Chem. C*, 2013, **117**, 15009–15019.
- 42.** Q. Du, M. Zheng, L. Zhang, Y. Wang, J. Chen, L. Xue, W. Dai, G. Ji and J. Cao, *Electrochim. Acta*, 2010, **55**, 3897.
- 43.** H. Jiang, J. Ma and C. Z. Li, *Adv. Mater.*, 2012, **24**, 4197– 4202.
- 44.** M. Q. Wu, J. H. Gao, S. R. Zhang and A. Chen, *J. Porous Mater.* 2006, **13**, 407–412.
- 45.** Y. Lin, N. Zhao, W. Nie and X. Ji, *J. Phys. Chem. C*, 2008, **112**, 16219.
- 46.** W. Sun and X. Chen, *J. Power Sources*, 2009, **193**, 924.

47. W. Sun and X. Chen, *J. Power Sources*, 2009, **193**, 924.
48. M. Shao, Z. Li, R. Zhang, F. Ning, M. Wei, D. G. Evans and X. Duan, *Small* 2015, **11(29)**, 3530-3538
49. S. Nejati, T. E. Minford, Y. Y. Smolin, K. K. S. Lau, *ACS Nano*, 2014, **8**, 5413–5422.
50. R. Ramachandran, M. Saranya, P. Kollu, B. P. C. Ragupathy, S. K. Jeong and A. N. Grace, *Electrochim. Acta*, 2015, **178**, 647–657.
51. N. Terasawa and K. Asaka, *Langmuir*, 2014, **30**, 14343–14351.
52. Y. Li, M. V. Zijll, S. Chiang and N. Pan, *J. Power Sources*, 2011, **196**, 6003.
53. A. Burke, *Electrochim. Acta*, 2007, **53**, 1083-1091.
54. Y. Lin, X. Wang, G. Qian and J. J. Watkins, *Chem. Mater.* 2014, **26**, 2128–2137.
55. Béguin F, Presser V, Balducci A, Frackowiak E. Carbons and electrolytes for advanced supercapacitors. *Advanced Materials*. 2014;26:2219-2251
56. Akinwolemiwa B, Peng C, Chen GZ. Redox electrolytes in supercapacitors. *Journal of the Electrochemical Society*. 2015;162:A5054-A5059
57. F. Wang, X. Wu, X. Yuan, Z. Liu, Y. Zhang, L. Fu, Y. Zhu, Q. Zhou, Y. Wu and W. Huang, *Chem. Soc. Rev.*, 2017, **46**, 6816–6854.
58. L. Suo, O. Borodin, T. Gao, M. Olguin, J. Ho, X. Fan, C. Luo, C. Wang and K. Xu, *Science*, 2015, **350**, 9367.
59. M. Rajkumar, C. T. Hsu, T. H. Wu, M. G. Chen, C. C. Hu, 2015, 527
60. S. Trasatti and G. Buzzanca, *J. Electroanal. Chem.*, 1971, **29**, 1–5.
61. C. Tang, Z. Tang, H. Gong, Hierarchically porous Ni-co oxide for high reversibility asymmetric full-cell supercapacitors, *J. Electrochem. Soc.* 159 (5) (2012) A651–A656.
62. C.-C. Hu, K.-H. Chang, M.-C. Lin, Y.-T. Wu, Design and tailoring of the nanotubular arrayed architecture of hydrous RuO<sub>2</sub> for next generation supercapacitors, *Nano Lett.* 6 (12) (2006) 2690–2695.
63. N. L. Wu, S. L. Kuo, M. H. Lee, *J. Power Sources* 104 (2002) 62–65.
64. I. D. Raistrick, in: J. McHardy, F. Luduig (Eds.), *The Electrochemistry of semiconductors and Electronics Processes and Devices*, 1992, Noyes, Park Ridge, NJ.
65. Y. Sato, K. Yomogida, T. Nanaumi, K. Kobayakawa, Y. Ohsawa, M. Kawai, *Electrochim. Solid State Lett.* 3, 113 (2000).
66. C. Lin, J. A. Ritter, B. N. Popov, *J. Electrochem. Soc.* 146, 3155 (1999).
67. Y. Takasu, T. Nakamura, H. Ohkawauchi, Y. Murakami, *J. Electrochem. Soc.* 144, 2601 (1997).
68. Y. G. Wang, Z. D. Wang, Y. Y. Xia, *Electrochimica Acta* 50, 5646 (2005).
69. Huang, H. S., K. H. Chang, N. Suzuki, Y. Yamauchi, C. C. Hu and K. C. W. Wu. 2013. Evaporation-Induced Coating of Hydrous Ruthenium Oxide on Mesoporous Silica Nanoparticles to Develop High-Performance Supercapacitors. *Small* 9 (15):2520-2526.
70. Wu, Z., L. Li, J. m. Yan and X. b. Zhang. 2017. Materials Design and System Construction for Conventional and New-Concept Supercapacitors. *Advanced Science* 4 (6):1600382
71. Wu, Z. S., D. W. Wang, W. Ren, J. Zhao, G. Zhou, F. Li and H. M. Cheng. 2010. Anchoring hydrous RuO<sub>2</sub> on graphene sheets for high-performance electrochemical capacitors. *Advanced Functional Materials* 20 (20):3595-3602.
72. Ardizzone, S., G. Fregonara and S. Trasatti. 1990. “Inner” and “outer” active surface of RuO<sub>2</sub> electrodes. *Electrochimica acta* 35 (1):263-267

- 73.**Hu, C.-C., W.-C. Chen and K.-H. Chang. 2004. How to achieve maximum utilization of hydrous ruthenium oxide for supercapacitors. *Journal of the Electrochemical Society* 151 (2):A281-A290.
- 74.**Naoi, K., S. Ishimoto, N. Ogihara, Y. Nakagawa and S. Hatta. 2009. Encapsulation of nanodot ruthenium oxide into KB for electrochemical capacitors. *Journal of the Electrochemical Society* 156 (1):A52-A59.
- 75.**Kim, Y.-T., K. Tadai and T. Mitani. 2005. Highly dispersed ruthenium oxide nanoparticles on carboxylated carbon nanotubes for supercapacitor electrode materials. *Journal of Materials Chemistry* 15 (46):4914-4921.
- 76.**Wu, Z. S., D. W. Wang, W. Ren, J. Zhao, G. Zhou, F. Li and H. M. Cheng. 2010. Anchoring hydrous RuO<sub>2</sub> on graphene sheets for high-performance electrochemical capacitors. *Advanced Functional Materials* 20 (20):3595-3602.
- 77.** Desai, B. D., Fernandes, J. B., & Dalal, V. N. K. (1985). Manganese dioxide — a review of a battery chemical Part II. Solid state and electrochemical properties of manganese dioxides. *Journal of Power Sources*, 16(1), 1-43
- 78.** Messaoudi, B., Joiret, S., Keddou, M., & Takenouti, H. (2001). Anodic behaviour of manganese in alkaline medium. *Electrochimica Acta*, 46(16), 2487-2498
- 79.**Li, S., L.-L. Yu, R.-B. Li, J. Fan and J.-T. Zhao. 2018. Template-free and room-temperature synthesis of 3D sponge-like mesoporous Mn<sub>3</sub>O<sub>4</sub> with high capacitive performance. *Energy Storage Materials* 11:176-183
- 80.**Li, R., Y. Wang, C. Zhou, C. Wang, X. Ba, Y. Li, X. Huang and J. Liu. 2015. Carbon-stabilized high-capacity ferroferric oxide nanorod array for flexible solid-state alkaline battery–supercapacitor hybrid device with high environmental suitability. *Advanced Functional Materials* 25 (33):5384-5394.
- 81.**Wei, W., X. Cui, W. Chen and D. G. Ivey. 2011. Manganese oxide-based materials as electrochemical supercapacitor electrodes. *Chemical Society Reviews* 40 (3):1697-1721
- 82.**Kim, S. J., I. Y. Kim, S. B. Patil, S. M. Oh, N. S. Lee and S. J. Hwang. 2014. Composition-Tailored 2 D Mn<sub>1-x</sub>Ru<sub>x</sub>O<sub>2</sub> Nanosheets and Their Reassembled Nanocomposites: Improvement of Electrode Performance upon Ru Substitution. *Chemistry—A European Journal* 20 (17):5132-5140
- 83.**Wang, J.-G., F. Kang and B. Wei. 2015. Engineering of MnO<sub>2</sub>-based nanocomposites for high-performance supercapacitors. *Progress in Materials Science* 74:51-124.
- 84.**Hu, Y., Y. Wu and J. Wang. 2018. Manganese-Oxide-Based Electrode Materials for Energy Storage Applications: How Close Are We to the Theoretical Capacitance? *Advanced materials* 30 (47):1802569.
- 85.**Zhang, Q. Z., D. Zhang, Z. C. Miao, X. L. Zhang and S. L. Chou. 2018. Research progress in MnO<sub>2</sub>-carbon based supercapacitor electrode materials. *Small* 14 (24):1702883
- 86.**Hu, Y., Y. Wu and J. Wang. 2018. Manganese-Oxide-Based Electrode Materials for Energy Storage Applications: How Close Are We to the Theoretical Capacitance? *Advanced materials* 30 (47):1802569
- 87.** Jian, X., S. Liu, Y. Gao, W. Zhang, W. He, A. Mahmood, C. M. Subramaniam, X. Wang, N. Mahmood and S. X. Dou. 2017. Facile Synthesis of Three-Dimensional Sandwiched MnO<sub>2</sub>@ GCs@ MnO<sub>2</sub> Hybrid nanostructured

Electrode for Electrochemical Capacitors. ACS applied materials & interfaces 9 (22):18872-18882

**88.** Bian, S.-W., Y.-P. Zhao and C.-Y. Xian. 2013. Porous MnO<sub>2</sub> hollow spheres constructed by nanosheets and their application in electrochemical capacitors. Materials Letters 111:75-77

**89.** Zhou, L., Z. Zhuang, H. Zhao, M. Lin, D. Zhao and L. Mai. 2017. Intricate hollow structures: controlled synthesis and applications in energy storage and conversion. Advanced materials 29 (20):1602914.

**90.** Yu, L., H. B. Wu and X. W. D. Lou. 2017. Self-templated formation of hollow structures for electrochemical energy applications. Accounts of chemical research 50 (2):293-301.

**91.** Yao, W., J. Wang, H. Li and Y. Lu. 2014. Flexible  $\alpha$ -MnO<sub>2</sub> paper formed by millimeter-long nanowires for supercapacitor electrodes. Journal of Power Sources 247:824-830.

**92.** Xia, H., J. Feng, H. Wang, M. O. Lai and L. Lu. 2010. MnO<sub>2</sub> nanotube and nanowire arrays by electrochemical deposition for supercapacitors. Journal of Power Sources 195 (13):4410-4413.

**93.** Zhai, T., S. Xie, M. Yu, P. Fang, C. Liang, X. Lu and Y. Tong. 2014. Oxygen vacancies enhancing capacitive properties of MnO<sub>2</sub> nanorods for wearable asymmetric supercapacitors. Nano Energy 8:255-263.

**94.** Wang, Z. and F. Wang. 2017. An innovative carbon template-induced approach to a graphene-like MnO<sub>2</sub> nanomesh with enhanced pseudocapacitance performance. Journal of Materials Chemistry A 5 (20):9709-9716

**95.** Qian, T., J. Zhou, N. Xu, T. Yang, X. Shen, X. Liu, S. Wu and C. Yan. 2015. On-chip supercapacitors with ultrahigh volumetric performance based on electrochemically co-deposited CuO/polypyrrole nanosheet arrays. Nanotechnology 26 (42):425402.

**96.** Zhu, C., L. Yang, J. K. Seo, X. Zhang, S. Wang, J. Shin, D. Chao, H. Zhang, Y. S. Meng and H. J. Fan. 2017. Self-branched  $\alpha$ -MnO<sub>2</sub>/ $\delta$ -MnO<sub>2</sub> heterojunction nanowires with enhanced pseudocapacitance. Materials Horizons 4 (3):415-420

**97.** Bag, S. and C. R. Raj. 2016. Facile shape-controlled growth of hierarchical mesoporous  $\delta$ -MnO<sub>2</sub> for the development of asymmetric supercapacitors. Journal of Materials Chemistry A 4 (21):8384-8394.

**98.** Lee, J. W., A. S. Hall, J.-D. Kim and T. E. Mallouk. 2012. A facile and template-free hydrothermal synthesis of Mn<sub>3</sub>O<sub>4</sub> nanorods on graphene sheets for supercapacitor electrodes with long cycle stability. Chemistry of Materials 24 (6):1158-1164.

**99.** Yeager, M. P., W. Du, Q. Wang, N. A. Deskins, M. Sullivan, B. Bishop, D. Su, W. Xu, S. D. Senanayake and R. Si. 2013. Pseudocapacitive Hausmannite Nanoparticles with (101) Facets: Synthesis, Characterization, and Charge-Transfer Mechanism. ChemSusChem 6 (10):1983-1992.

**100.** Y.F. Lee, K.H. Chang, C.C. Hu, Y.H. Chu, J. Power Sources 206(2012) 469–475.

**101.** L. Wang, M. Huang, S. Chen, L. Kang, X. He, Z. Lei, F. Shi, H. Xu, Z.-H. Liu,  $\delta$ -MnO<sub>2</sub> nanofibre/single-walled carbon nanotube hybrid film for all-solid-state flexible supercapacitors with high performance, J. Mater. Chem. A 5 (36) (2017) 19107–19115.

- 102**D. Zhou, H. Lin, F. Zhang, H. Niu, L. Cui, Q. Wang, F. Qu, Freestanding MnO<sub>2</sub> nanoflakes/porous carbon nanofibres for high-performance flexible supercapacitor electrodes, *Electrochim. Acta* 161 (2015) 427–435.
- 103**.K. Xu, S. Li, J. Yang, J. Hu, Hierarchical hollow MnO<sub>2</sub> nanofibres with enhanced supercapacitor performance, *J. Colloid Interface Sci.* 513 (2018) 448–454
- 104**.Liu, J., Essner, J., & Li, J. (2010). Hybrid Supercapacitor Based on Coaxially Coated Manganese Oxide on Vertically Aligned Carbon Nanofiber Arrays. *Chem. Mater.*, 22(17), 5022-5030.
- 105**. Sarkar, A., Kumar Satpati, A., Kumar, V., & Kumar, S. (2015). Sol-gel synthesis of manganese oxide films and their predominant electrochemical properties. *Electrochimica Acta*, 167, 126-131
- 106**. Yadav, A. A., Jadhav, S. N., Chougule, D. M., Patil, P. D., Chavan, U. J., & Kolekar, Y. D. (2016). Spray deposited Hausmannite Mn<sub>3</sub>O<sub>4</sub> thin films using aqueous/organic solvent mixture for supercapacitor applications. *Electrochimica Acta*, 206, 134-142
- 107**. Broughton, J. N., & Brett, M. J. (2004). Investigation of thin sputtered Mn films for electrochemical capacitors. *Electrochimica Acta*, 49(25), 4439-4446
- 108**. Toupin, M., Brousse, T., & Bélanger, D. (2004). Charge Storage Mechanism of MnO<sub>2</sub> Electrode Used in Aqueous Electrochemical Capacitor. *Chem. Mater.*, 16(16), 3184-3190
- 109**. Pang, S. C., Anderson, M. A., & Chapman, T. W. (2000). Novel Electrode Materials for Thin-Film Ultracapacitors: Comparison of Electrochemical Properties of Sol-Gel-Derived and Electrodeposited Manganese Dioxide. *Journal of The Electrochemical Society*, 147(2), 444-450
- 110**. Chen, S.-H., Wu, C.-H., Fang, A., & Lin, C.-K. (2016). Effects of adding different morphological carbon nanomaterials on supercapacitive performance of sol-gel manganese oxide films. *Ceramics International*, 42(4), 4797-4805
- 111**. Wu, C.-H., Ma, J.-S., & Lu, C.-H. (2012). Synthesis and characterization of nickel-manganese oxide via the hydrothermal route for electrochemical capacitors. *Current Applied Physics*, 12(4), 1190-1194
- 112**. Chang, J.-K., Lee, M.-T., Huang, C.-H., & Tsai, W.-T. (2008). Physicochemical properties and electrochemical behavior of binary manganese-cobalt oxide electrodes for supercapacitor applications. *Mater. Chem. Phys.*, 108(1), 124-131
- 113**. Singh, A. K., Sarkar, D., Karmakar, K., Mandal, K., & Khan, G. G. (2016). High-Performance Supercapacitor Electrode Based on Cobalt Oxide-Manganese Dioxide-Nickel Oxide Ternary 1D Hybrid Nanotubes. *ACS Applied Materials & Interfaces*, 8(32), 20786-20792
- 114**. Hong, S., Lee, S., & Paik, U. (2014). Core-Shell Tubular Nanostructured Electrode of Hollow Carbon Nanofiber/Manganese Oxide for Electrochemical Capacitors. *Electrochimica Acta*, 141, 39-44
- 115**. Yu, S., V. M. H. Ng, F. Wang, Z. Xiao, C. Li, L. B. Kong, W. Que and K. Zhou. 2018. Synthesis and application of iron-based nanomaterials as anodes of lithium-ion batteries and supercapacitors. *Journal of Materials Chemistry A* 6 (20):9332-9367.
- 116**. Ma, J., X. Guo, Y. Yan, H. Xue and H. Pang. 2018. FeO<sub>x</sub>-Based Materials for Electrochemical Energy Storage. *Advanced Science* 5 (6):1700986.
- 117**. Li, R., Y. Wang, C. Zhou, C. Wang, X. Ba, Y. Li, X. Huang and J. Liu. 2015. Carbon-stabilized high-capacity ferroferric oxide nanorod array for flexible solid-

state alkaline battery–supercapacitor hybrid device with high environmental suitability. *Advanced Functional Materials* 25 (33):5384-5394.

**118.**Liu, J., M. Chen, L. Zhang, J. Jiang, J. Yan, Y. Huang, J. Lin, H. J. Fan and Z. X. Shen. 2014. A flexible alkaline rechargeable Ni/Fe battery based on graphene foam/carbon nanotubes hybrid film. *Nano Letters* 14 (12):7180-7187.

**119.**Xia, Q., M. Xu, H. Xia and J. Xie. 2016. Nanostructured Iron Oxide/Hydroxide-Based Electrode Materials for Supercapacitors. *ChemNanoMat* 2 (7):588-600.

**120.**Sakurai, S., A. Namai, K. Hashimoto and S.-i. Ohkoshi. 2009. First observation of phase transformation of all four Fe<sub>2</sub>O<sub>3</sub> phases ( $\gamma \rightarrow \epsilon \rightarrow \beta \rightarrow \alpha$ -phase). *Journal of the American Chemical Society* 131 (51):18299-18303.

**121.**Danno, T., D. Nakatsuka, Y. Kusano, H. Asaoka, M. Nakanishi, T. Fujii, Y. Ikeda and J. Takada. 2013. Crystal structure of  $\beta$ -Fe<sub>2</sub>O<sub>3</sub> and topotactic phase transformation to  $\alpha$ -Fe<sub>2</sub>O<sub>3</sub>. *Crystal Growth & Design* 13 (2):770-774.

**122.**Li, T., H. Yu, L. Zhi, W. Zhang, L. Dang, Z. Liu and Z. Lei. 2017. Facile electrochemical fabrication of porous Fe<sub>2</sub>O<sub>3</sub> nanosheets for flexible asymmetric supercapacitors. *The Journal of Physical Chemistry C* 121 (35):18982-18991.

**123.**Lu, X., Y. Zeng, M. Yu, T. Zhai, C. Liang, S. Xie, M. S. Balogun and Y. Tong. 2014. Oxygen-deficient hematite nanorods as high-performance and novel negative electrodes for flexible asymmetric supercapacitors. *Advanced materials* 26 (19):3148-3155.

**124.**Tang, Q., W. Wang and G. Wang. 2015. The perfect matching between the low-cost Fe<sub>2</sub>O<sub>3</sub> nanowire anode and the NiO nanoflake cathode significantly enhances the energy density of asymmetric supercapacitors. *Journal of Materials Chemistry A* 3 (12):6662-6670.

**125.**Shivakumara, S., T. R. Penki and N. Munichandraiah. 2014. High specific surface area  $\alpha$ -Fe<sub>2</sub>O<sub>3</sub> nanostructures as high performance electrode material for supercapacitors. *Materials Letters* 131:100-103.

**126.**Yang, P., Y. Ding, Z. Lin, Z. Chen, Y. Li, P. Qiang, M. Ebrahimi, W. Mai, C. P. Wong and Z. L. Wang. 2014. Low-cost high-performance solid-state asymmetric supercapacitors based on MnO<sub>2</sub> nanowires and Fe<sub>2</sub>O<sub>3</sub> nanotubes. *Nano Letters* 14 (2):731-736.

**127.**Liu, T., Y. Ling, Y. Yang, L. Finn, E. Collazo, T. Zhai, Y. Tong and Y. Li. 2015. Investigation of hematite nanorod–nanoflake morphological transformation and the application of ultrathin nanoflakes for electrochemical devices. *Nano Energy* 12:169-17

**128.** Li, T., H. Yu, L. Zhi, W. Zhang, L. Dang, Z. Liu and Z. Lei. 2017. Facile electrochemical fabrication of porous Fe<sub>2</sub>O<sub>3</sub> nanosheets for flexible asymmetric supercapacitors. *The Journal of Physical Chemistry C* 121 (35):18982-18991.

**129.**Zheng, X., X. Yan, Y. Sun, Y. Yu, G. Zhang, Y. Shen, Q. Liang, Q. Liao and Y. Zhang. 2016. Temperature-dependent electrochemical capacitive performance of the  $\alpha$ -Fe<sub>2</sub>O<sub>3</sub> hollow nanoshuttles as supercapacitor electrodes. *Journal of colloid and interface science* 466:291-296

- 130.** Mo, Z., C. Zhang, R. Guo, S. Meng and J. Zhang. 2011. Synthesis of Fe<sub>3</sub>O<sub>4</sub> nanoparticles using controlled ammonia vapor diffusion under ultrasonic irradiation. *Industrial & Engineering Chemistry Research* 50 (6):3534-3539.
- 131.** Guan, G., L. Yang, Q. Mei, K. Zhang, Z. Zhang and M.-Y. Han. 2012. Chemiluminescence switching on peroxidase-like Fe<sub>3</sub>O<sub>4</sub> nanoparticles for selective detection and simultaneous determination of various pesticides *Analytical chemistry* 84 (21):9492-9497..
- 132.** Li, F., H. Chen, X. Y. Liu, S. J. Zhu, J. Q. Jia, C. H. Xu, F. Dong, Z. Q. Wen and Y. X. Zhang. 2016. Low-cost high-performance asymmetric supercapacitors based on Co<sub>2</sub>AlO<sub>4</sub>@MnO<sub>2</sub> nanosheets and Fe<sub>3</sub>O<sub>4</sub> nanoflakes. *Journal of Materials Chemistry A* 4 (6):2096-2104
- 133.** T. Nathan, A. Aziz, A.F. Noor, S.R.S. Prabaharan, J. *Solid State Electrochem.* 12, 1009 (2008).
- 134.** D. Zhao, W. Zhou, H. Li, *Chem. Mater.* 19, 3882 (2007).
- 135.** J. W. Lee, T. Ahn, J. H. Kim, J. M. Ko, J. D. Kim, *Electrochimica Acta* 56, 4857 (2011).
- 136.** T.W. Kim, S.-J. Hwang, S.H. Jhung, J.-S. Chang, H. Park, W. Choi, J.H. Choy, *Adv. Mater.* 20, 542 (2008).
- 137.** J.S.E.M. Svensson, C.G. Granqvist, *Appl. Phys. Lett.* 49, 1568 (2009).
- 138.** B. Varghese, M.V. Reddy, Y.W. Zhu, C.S. Lit, T.C. Hoong, G.V. Subba Rao, B.V.R. Chowdari, A.T.S. Wee, C.T. Lim, C.- H. Sow, *Chem. Mater.* 20, 3367 (2008).
- 139.** X. Li, J.P. Liu, X.X. Ji, J. Jiang, R.M. Ding, Y.Y. Hu, A.Z. Hu, X.T. Huang, *Sens. Actuators B* 147, 247 (2010).
- 140.** D.Y. Han, H.Y. Yang, C.B. Shen, X. Zhou, F.H. Wang, *Powder Technol.* 147, 116 (2004).
- 141.** C.K. Xu, K.Q. Hong, S. Liu, G.H. Wang, X.N. Zhao, *J. of Cryst. Growth* 255, 312. (2003). ISSN 2320-5407 *International Journal of Advanced Research* (2016), Volume 4, Issue 3, 1943-1975 1979
- 142.** Y.J. Zhan, C.R. Yin, C.L. Zheng, W.Z. Wang, G.H. Wang, *J. of Solid State Chem.* 177, 2284 (2004).
- 143]** H.A. Pang, Q.Y. Lu, Y.Z. Zhang, Y.C. Li, F. Gao, *Nanoscale* 2, 922 (2010).
- 144.** W.Z. Wang, Y.K. Liu, C.K. Xu, C.L. Zheng, G.H. Wang, *Chem. Phys. Lett.* 362,122. (2002).
- 145.** S.A. Needham, G.X. Wang, H.K. Liu, *J. of Power Sources* 159, 257 (2006).
- 146]** X. M. Ni, Y.F. Zhang, D.Y. Tian, H.G. Zheng, X.W. Wang, *J. of Cryst. Growth* 306, 421 (2007).
- 147.** M. Zhang, G.J. Yan, Y.G. Hou, C.H. Wang, *J. of Solid State Chem.* 182, 1210 (2009).
- 148]** W. Zhou, L. Ge, Z. Chen, F. Liang, H. Xu., J. Motuzas, A. Julbe, Z. Zhu, *Chemistry of Materials* 23, 4198 (2011).
- 149]** G.X. Pan, X. Xia, F. Cao, P.S. Tang, H.F. Chen, *Electrochimica Acta* 63, 340 (2012).
- 150.** H.Y. Wu and H. W. Wang, *Int. J. Electrochem. Sci.*, 2012, **7**, 4405 – 4417
- 151.** M. S. Wu, Y. A. Huang, C. H. Yang and J. J. Jow, *Int. J. Hydrogen Energy*, 2007, **32**, 4153 – 4159
- 152.** R. M. Kore, R. S. Mane, M. Naushad, M. R. Khan and B. J. Lokhande, *RSC Adv.*, 2016, **6**, 24478–24483

- 153.** A. D. Jagadale, V. S. Kumbhar, D. S. Dhawale and C. D. Lokhande, *J. Electroanal. Chem.*, 2013, **704**, 90–95
- 154.** G. R. Fu, Z. A. Hu, L. J. Xie, X. Q. Jin, Y. L. Xie, Y. X. Wang, Z. Y. Zhang, Y. Y. Yang and H. Y. Wu, *Int. J. Electrochem. Sci.*, 2009, **4**, 1052-106
- 155.** Maiti S, Pramanik A, DhawaTSreemany M, Mahanty S. Bi-meta organic framework derived nicke manganese oxide spinel for lithium-io battery anode. *Materials Science an Engineering: B*. 2018;229:27-36
- 156.** Ngo YLT, Sui L, Ahn W, Chung JS, Hur SH. NiMn2O4 spinel binary nanostructure decorated on threedimensiona reduced graphene oxid hydrogel for bifunctionaaterials on-enzymatic glucose sensor *Nanoscale*. 2017;9:19318-19327
- 157.** V. D. Patake, S. S. Joshi, C. D. Lokhande and O. S. Joo, *Mater. Chem. Phys*, 2009, **114**, 6–9
- 158.** D. P. Dubal, G. S. Gund , C. D. Lokhande and R. Holze, *Mater. Res. Bull.*, 2013, **48**, 923–928
- 159.** Y. Li, S. Chang, X. Liu, J. Huang, J. Yin, G. Wang and D. Cao, *Electrochim. Acta*, 2012, **85**, 393– 398
- 160.** T. S. Ghadge and B. J. Lokhande, *J. Mater. Sci.*, 2016, **51(21)**, 9879-9888.
- 161** H. Y. Lee and J. B, *Solid State Chem.*, 1999,**48**, 81-84.
- 162** K. K. Upadhyay, T. Nguyen, T. M. Silva, M. J. Carmezim, and M. F. Montemor, *Electrochim. Acta*, 2016, **12**, 106
- 163.** T. Gujar, V. Shinde, C. Lokhande and S. H. Han, *J. Power Sources*, 2006, **161**, 1479-1485.
- 164.** K. R. Prasad, N. Miura, *Electrochem. Commun.*, 2004, **6**, 849-852
- 165.** A. Tamilselvan and S. Balakumar, *Ionics*, 2016, **22(1)**, 99-105.
- 166.** K. R. Prasad, K. Koga, N. Miura, *Chem. Mater.*, 2004, **16**, 1845-1848
- 167** J.H. Zheng, R.M. Zhang, P.F. Yu, X.G. Wang, Binary transition metal oxides (BTMO)(Co-Zn, Co-Cu) synthesis and high supercapacitor performance, *J. Alloys Compd.*772 (2019) 359–365.
- 168**Z. Zhang, Z. Xu, Z. Yao, Y. Meng, Q. Xia, D. Li, Z. Jiang, Ultrahigh capacitance of TiO2 nanotube arrays/C/MnO2 electrode for supercapacitor, *J. Alloys Compd.* 805 (2019)396–403.
- [**169**] S. Mothkuri, S. Chakrabarti, H. Gupta, B. Padya, T.N. Rao, P.K. Jain, Synthesis of MnO2 nano-flakes for high performance supercapacitor application, *Materials Today: Proceedings* (2019).
- [**170**] T.-F. Yi, J. Mei, B. Guan, P. Cui, S. Luo, Y. Xie, Y. Liu, Construction of spherical NiO@ MnO2 with core-shell structure obtained by depositing MnO2 nanoparticles on NiO nanosheets for high-performance supercapacitor, *Ceram. Int.* 46 (2020) 421–429.
- [**171**] J. Lin, Y.Yan, H.Wang, X. Zheng, Z. Jiang, Y.Wang, J. Qi, J. Cao,W. Fei, J. Feng,Hierarchical Fe2O3 and NiO nanotube arrays as advanced anode and cathode electrodes for high-performance asymmetric supercapacitors, *J. Alloys Compd.* 794 (2019) 255–260.

**172]** P.Wang, H. Zhou, C.Meng, Z. Wang, K. Akhtar, A. Yuan, Cyanometallicframeworkderived hierarchical Co<sub>3</sub>O<sub>4</sub>-NiO/graphene foam as high-performance binder-free electrodes for supercapacitors, Chem. Eng. J. 369 (2019) 57–60